A thesis submitted in partial fulfillment of the requirements for the degree of Master of Science

Modulation of the Ago2-Associated microRNA Induced Silencing Complex during Long-Term Potentiation in the Rat Dentate Gyrus *in Vivo*

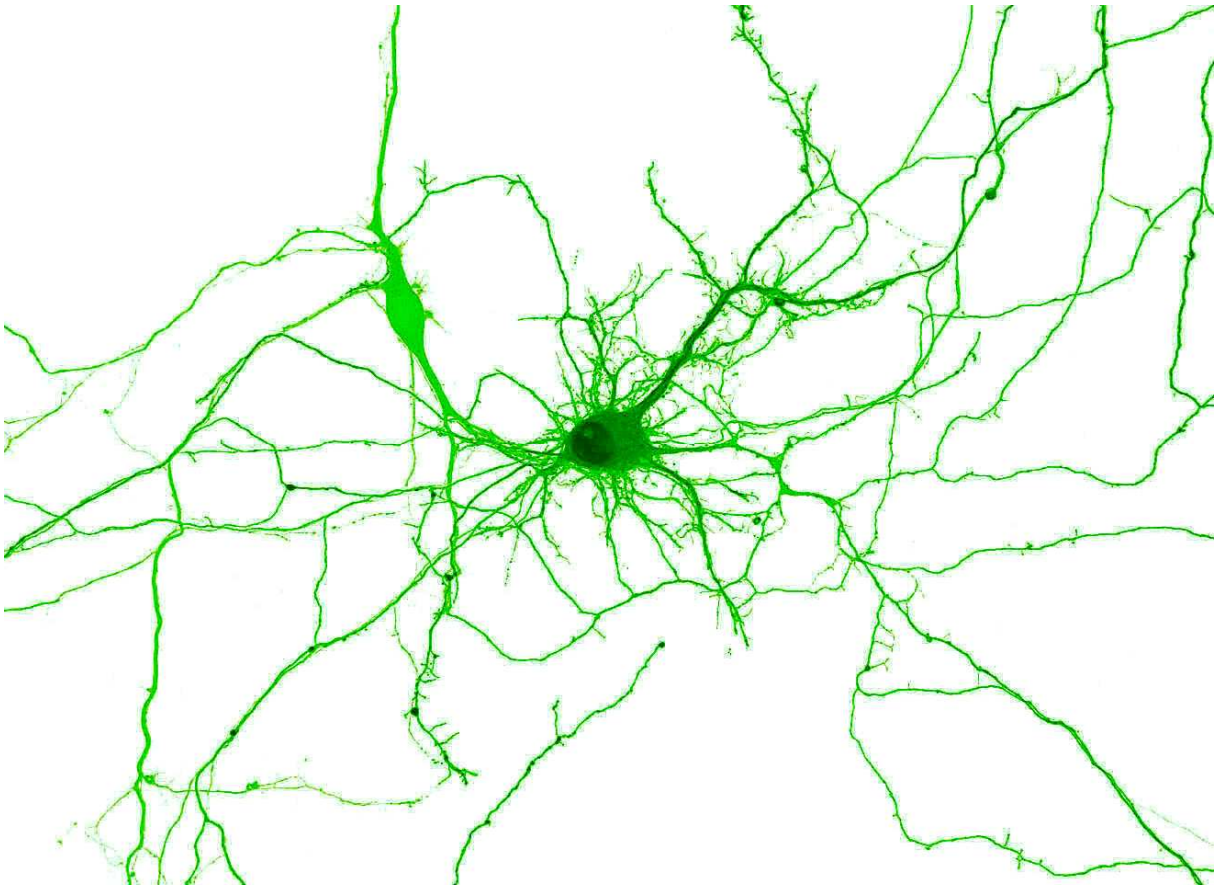

Christel Marie Vieuille

University of Bergen, Norway
Department of Biomedicine
May 2012

Preface

The cover shows a confocal live image of a hippocampal neuron transfected with the Dendra2 fluorescent reporter protein. The colors have been inverted and the hue adjusted. All the work was performed by Adrian Szum. Printed with permission.

Many of the figures in this document are color images and are best viewed as a PDF-file or in a color printout.

"There is a foolish corner in the brain of the wisest man."
-Aristotle

Acknowledgements

This thesis is part of the degree of Master of Science in Medical Biology, specialization in Human Physiology. The work was conducted at the Department of Biomedicine, University of Bergen, during the period of August 2011 to June 2012.

First, I would like to express my sincere gratitude to my supervisor, Professor Clive Bramham, for invaluable advice, and for providing such an excellent research environment. Also, he made me feel welcome in the group, and his catchy enthusiasm for neuroscience made me want to stay in the field.

It is a pleasure for me to thank my lab supervisor, Tambu, whose guidance and support have gone beyond any expectations. She has helped me develop skills in both writing and laboratory work, and has offered good advice all the countless times I came knocking on her door. I would also like to thank Balu for taking the time to teach me immunoprecipitation, and for answering innumerable questions from me. Thank you both for your kindness, cheerfulness and friendship.

Many thanks to Birgitte for producing all the tissue used in my experiments, to Craig for teaching me proteomics and cell culture, to Jonathan for useful commentaries on my writing, and to Olav at PROBE for performing mass spectrometry.

I also wish to thank the remaining members of the lab, Adrian S., Adrian T., Ashraf, Deb, Karin, Manja, Maria, May Lillian, Ogi, Oleksii, Sjoukje, Sue and Torhild. You have all been most helpful and kind, and it has been a pleasure working with you. Also, thanks to Karen Lise for the coffee.

Thanks to my fellow master students for good times during this busy period. And special thanks to old and new friends and roommates in Oslo and Bergen, your friendship means the world to me.

Enfin, merci à toute ma famille, spécialement Papa, Maman, Yann et Andréas, pour m'avoir toujours encouragé à poursuivre mes rêves et ambitions, aussi bien dans mes études que dans la vie en général.

Bergen, May 2012

Christel Vieuille

Christel Vieuille

Abstract

Synaptic plasticity is defined as the ability of a neuronal synapse to change in strength, and is believed to be the basis of learning and memory. An example of synaptic plasticity, by far the most studied, is long-term potentiation (LTP): a stable, activity-induced increase in synaptic efficacy. LTP requires *de novo* gene expression, protein synthesis and protein degradation. Transcriptional and post-transcriptional regulation controls new protein expression. In the past decade, small non-coding RNAs called microRNAs have emerged as key regulators of translation. MicroRNAs bind to target mRNAs by complementary binding and recruit a protein complex to mediate mRNA silencing. This complex is known as the microRNA-induced silencing complex (miRISC). The goals of this study were to investigate the composition of the miRISC in the rat dentate gyrus *in vivo*, to study modulation of the miRISC during LTP, and to uncover new candidate binding partners of Ago2. LTP was induced by HFS of the medial perforant path. The miRISC was isolated by immunoprecipitation of its core component, the protein Argonaute 2 (Ago2). Five proteins thought to bind Ago2 were analyzed by co-immunoprecipitation with Ago2. These proteins were GW182, the RNase III enzyme, Dicer, the RNA-binding protein, FMRP, and the RNA helicases, MOV10 and DDX6. DDX6 was the only protein found to be reliably associated with Ago2, even though all the proteins were detected in association with Ago2 in HEK cells expressing EGFP-Ago2. DDX6 was non-significantly dissociated from Ago2 during LTP. In the total lysate, none of the analyzed proteins were significantly modulated during LTP. Nevertheless, Argonaute 2 and GW182 were non-significantly upregulated, and MOV10 was non-significantly downregulated during LTP. The study does not show a significant remodeling of the miRISC during LTP, but neither does it exclude this possibility. Immunoprecipitated samples were analyzed by mass spectrometry. New candidate Ago2 binding partners were uncovered, such as the proteins DDX1 and FXR1, homologs of DDX6 and FMRP. A protein important for translation, poly-A-binding protein 1 (PABP1), was also detected.

Table of contents

List of abbreviations

Ago2	Argonaute-2 protein
AMPA	α-amino-3-hydroxy-5-methyl-4-isoxazolepropionate
AMPAR	α-amino-3-hydroxy-5-methyl-4-isoxazolepropionate receptor
AP5	(2*R*)-amino-5-phosphonovaleric acid
Arc	Activity-regulated cytoskeleton-associated protein
Arg3.1	Activity-regulated gene 3.1
BCA	Bicinchoninic acid
BDNF	Brain-derived neurotrophic factor
CA	Cornu ammonis, Ammon's horn, hippocampus proper
CaMKII	Calcium/calmodulin-dependent protein kinase II
cAMP	Cyclic adenosine monophosphate
CPP	(RS)-3-2(2-Carboxypiperazin-4-yl)-propyl-1-phosphonic acid
CREB	cAMP response-element binding protein
CYFIP	Cytoplasmic fragile-X mental retardation interacting protein
DDX6	DEAD (Asp-Glu-Ala-Asp) box polypeptide 6
EGFP	Enhanced green fluorescent protein
E-LTP	Early phase of long-term potentiation
EPSP	Excitatory post-synaptic potential
ERK	Extracellular signal-regulated kinase
FMRP	Fragile-X mental retardation protein
GABA	Gamma amino butyric acid
GW182	Glycine-tryptophan protein of 182 kDa
HEK	Human embryonic kidney
HFS	High-frequency stimulation
hnRNP	Heterogeneous nuclear ribonucleoprotein
L-LTP	Late phase of long-term potentiation
LTD	Long-term depression
LTP	Long-term potentiation
MAPK	Mitogen-activated protein kinase
mGluR	Metabotropic glutamate receptor
miPDC	miRNA precursor deposit complex
miRISC	microRNA-induced silencing complex
miRLC	microRNA loading complex
miRNA	microRNA
MOV10	Moloney leukemia virus 10 protein
mRNA	Messenger RNA
NMDA	N-methyl-D-aspartate
NMDAR	N-methyl-D-aspartate receptor
PABP	Poly-A-binding protein
PKA	Protein kinase A, cAMP-dependent protein kinase
PKC	Protein kinase C
RNA	Ribonucleic acid
RNP	Ribonucleoprotein
TRBP	Transactivation-responsive RNA binding protein
UTR	Untranslated region

1 Introduction

Learning and memory are remarkable faculties of the brain, and the mechanisms underlying them have puzzled scientists for years. A mechanism thought to be involved in new memory formation is synaptic plasticity, the ability of a neuronal synapse to change in strength (Bliss et al., 2003). Studying synaptic plasticity may be important for future research on diseases of cognition such as Alzheimer's disease. To understand synaptic plasticity, one must start by understanding major building blocks of our brain, namely neurons.

1.1 Neurons and synapses

According to Ramón y Cajal's 'neuron doctrine' postulated in 1888, neurons are the structural and functional units making up our central nervous system. Cajal noted that neurons are polarized cells, and suggested that they convey information in only one direction (Andersen et al., 2007). The information is transmitted in the form of electrical pulses called *action potentials*. In 1897, Sherrington proposed that neurons are linked together by functional junctions, eventually named synapses. Synapses are now recognized as the principal sites of interneuronal communication. In chemical synapses, chemical *neurotransmitters* transmit the signals from one neuron to the next, via intercellular gaps called synaptic clefts. Chemical synapses can be either excitatory or inhibitory, depending on the type of neurotransmitter produced by the presynaptic neuron. Gamma-aminobutyric acid (GABA) is an inhibitory neurotransmitter, whereas glutamate is an excitatory one. Many neurons can be linked together to convey information between different brain areas, forming a circuit. A major theme of current research, and a subject of this thesis, is how synapses and neuronal circuits can change to store information, such as during memory storage. This thesis addresses only excitatory glutamatergic synapses.

1.2 Learning and memory

Learning, the process for acquisition of information altering behavior, knowledge or internal representation, may result in *memory*, the retention of such information. Memory is not a single faculty, but is composed of distinct systems. *Immediate memory* refers to short-term storage of sensory information. *Working memory* is the capacity to retain this information temporarily during the processing of a task. *Long-term memory* is the long-term storage of

information, achieved through the process of *consolidation*. It can last for hours, days, month or even years, and can be recalled at any moment, although reconsolidation may be necessary for retaining a specific memory. Long-term memory comprises different systems. The two main subordinate systems are *declarative (explicit) memory* and *nondeclarative (implicit) memory*. Declarative memory is a conscious representational recollection of facts and events, such as "Oslo is the capital of Norway" and "I went skiing yesterday". Nondeclarative memory refers to acquired skills expressed through performance, such as riding a bicycle or using chopsticks (Dudai, 2004; Squire, 2004). The hippocampus is a brain structure necessary for declarative memory formation (Martin et al., 2000; Neves et al., 2008).

1.3 The hippocampal formation

The *hippocampal formation* (Figure 1.1) is part of the *limbic system*, a phylogenetically old part of the cortex dealing with emotions and subconscious processes. Two major theories currently describe hippocampal function. First, the hippocampus has a time-limited involvement in the formation of declarative memory. Second, the hippocampus is involved in the formation of cognitive maps used for spatial navigation, or *spatial memory* (Andersen et al., 2007).

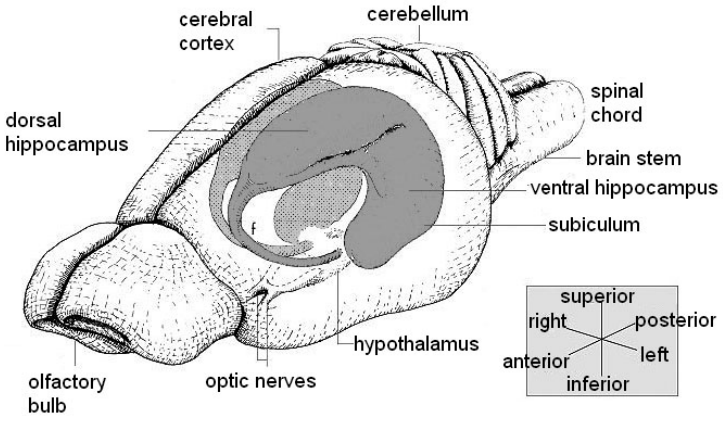

Figure 1.1 | The hippocampal formation in the rat brain. (Figure modified from Cheung and Cardinal, 2005)

The hippocampus is a bilateral structure, located between the cerebral cortex and the thalamus. As in humans, the rat hippocampus comprises the following structures: the subiculum, entorhinal cortex, dentate gyrus and cornu ammonis fields 1-3 (CA1, CA2, CA3). Neurons and fibers of the hippocampus are arranged in clear cut laminae. The principal cells of the dentate gyrus are the *granule cells*. These cells are densely packed and linearly arranged to form the granule cell layer. The primary cells of the CA region are the *pyramidal cells* (Andersen et al., 2007).

The main neural pathway of the hippocampus is the *trisynaptic circuit* (Figure 1.2), which is excitatory glutamatergic at every synapse. The entorhinal cortex conveys sensory information processed by the hippocampus back and forth to the neocortex. Granule cells of the dentate gyrus receive sensory information from layer II of the entorhinal cortex via the perforant path, forming a first synapse. The granule cells' axons, called mossy fibers, project to CA3 pyramidal cells, themselves innervating CA1 pyramidal cells through Schaffer collaterals. Return projections to the entorhinal cortex come from the CA1 and subiculum (Andersen et al., 2007; Neves et al., 2008).

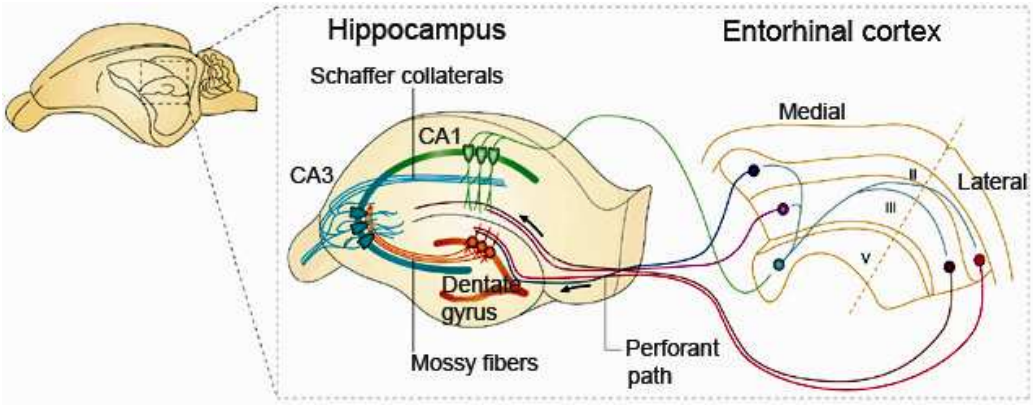

Figure 1.2 | The trisynaptic circuit. Here shown in the rat brain. The main signaling pathway of the hippocampus forms a loop. The entorhinal cortex conveys information to the granule cells of the dentate gyrus through the perforant path. Mossy fibers connect the granule cells to the pyramidal cells in the CA3 region, forming a second synapse. Then, Schaffer collaterals innervate CA1 pyramidal cells. Fibers from this region and the subiculum project back to the entorhinal cortex (Figure modified from Neves et al., 2008).

1.4 Synaptic plasticity

In 1949, Donald Hebb postulated a hypothesis describing synaptic plasticity, stating that:

> *When an axon of cell A is near enough to excite a cell B and repeatedly or persistently takes part in firing it, some growth process or metabolic change takes place in one or both cells such that A's efficiency, as one of the cells firing B, is increased.*

This activity-dependent ability of a synapse to change in strength is now widely assumed to be the basis of learning and memory. Synaptic plasticity is an attractive mechanism for learning and memory because its induction is rapid and associative, and its expression is input specific and persistent, much like memory itself (Bliss and Collingridge, 1993; Martin et al., 2000; Medina and Izquierdo, 1995). Experiments using different techniques, such as *in vivo* electrophysiological recordings, mutant mice and pharmacological treatment, show

similarities between LTP and memory (Medina and Izquierdo, 1995). In 2000, Martin et al. combined several ideas into a single synaptic plasticity and memory hypothesis. They summarized that:

> *Activity-dependent synaptic plasticity is induced at appropriate synapses during memory formation and is both necessary and sufficient for the information storage underlying the type of memory mediated by the brain area in which that plasticity is observed.*

Martin et al. (2000) investigated the validity of this hypothesis and concluded that synaptic plasticity may be necessary for learning and memory, but probably not sufficient. There are two main forms of synaptic plasticity: short- and long-term plasticity. Facilitation, depression and post-tetanic potentiation are examples of short-term plasticity, lasting seconds or less. Long-term potentiation (LTP) and long-term depression (LTD) are forms of long-term plasticity, lasting minutes, hours, days or months (Andersen et al., 2007). LTP is by far the most studied form of synaptic plasticity.

1.5 Long-term potentiation

LTP was first described by Bliss and Lømo in 1973. LTP occurs throughout the brain, but is most studied in the hippocampus, perhaps because of the hippocampus' involvement in learning and memory, and its neat laminar arrangement. LTP can be divided into two subsequent temporal phases known as *early-phase LTP* (E-LTP) and *late-phase LTP* (L-LTP) (Figure 1.3).

Figure 1.3 | The phases of LTP. Induction of LTP is triggered by high-frequency stimulation (HFS) of an afferent neuron, which causes an excitatory post-synaptic potential (EPSP), in turn leading to activation of several kinases. Early phase LTP (E-LTP) consists of modifications of preexisting proteins at the synapse by activated kinases. This nascent, short-lived potentiation may then be maintained through a process of consolidation, which depends on new gene expression and protein synthesis, giving rise to late phase LTP (L-LTP).

1.5.1 Induction of LTP

LTP can be N-methyl-D-aspartate receptor (NMDAR)-dependent or NMDAR-independent (Bliss et al., 2003). NMDAR-dependent LTP is the most prevalent form of LTP. Metabotropic glutamate receptors (mGluRs) may be involved in the induction of LTP, but play a more important role in LTD (Andersen et al., 2007; Medina and Izquierdo, 1995; Peng et al., 2011). Both electrical high-frequency stimulation (HFS) and application of pharmacological agents such as the neurotrophin brain-derived neurotrophic factor (BDNF) can induce LTP (Bliss and Lomo, 1973; Bramham and Messaoudi, 2005). LTP induced by HFS is NMDAR-dependent, whereas BDNF-induced LTP is NMDAR-independent (Messaoudi et al., 2002). HFS induces the release of glutamate, the brain's most prevalent excitatory neurotransmitter, into the synaptic cleft (Figure 1.4). In NMDAR-dependent LTP, glutamate binds to α-amino-3-hydroxy-5-methyl-4-isoxazolepropionate receptors (AMPARs) and NMDARs on the postsynaptic membrane. Glutamate binding to AMPARs leads to rapid influx of sodium ions (Na^+) into the postsynaptic spine, causing depolarization of the membrane. This excitatory post-synaptic potential (EPSP) relieves the magnesium ion (Mg^{2+}) blockage of the NMDARs, allowing influx of calcium ions (Ca^{2+}). Ca^{2+} may also be released from intracellular stores, and enter the spine through voltage-dependent Ca^{2+} channels. Ca^{2+} contributes to induce the early phase of LTP by activation of Ca^{2+}-dependent enzymes (Bliss and Collingridge, 1993; Peng et al., 2011).

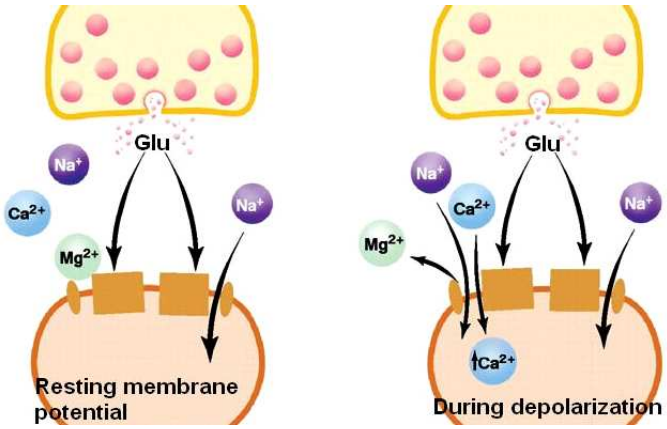

Figure 1.4 | Induction phase of NMDAR-dependent LTP. HFS-induced glutamate release into the synaptic cleft leads to glutamate binding to AMPARs and NMDARs. Na^+ influx through AMPARs depolarizes the membrane, allowing relief of the NMDARs' Mg^{2+} blockage. Ca^{2+} enters the spine through the open NMDARs and may induce LTP (Figure from Malenka and Nicoll, 1999).

1.5.2 Early phase LTP

E-LTP is in great part triggered by Ca^{2+}-sensitive protein kinases, such as protein kinase C (PKC), calcium/calmodulin-dependent protein kinase II (CaMKII), and mitogen-activated protein kinase (MAPK). PKC may for example increase Ca^{2+} influx through voltage-gated channels. CaMKII is a kinase known to phosphorylate AMPARs, increasing their function,

and causing AMPARs stored in intracellular vesicles to relocalize to the synaptic membrane (Malenka and Bear, 2004; Peng et al., 2011).

Retrograde messengers may be involved in communication between the pre- and post-synaptic site of LTP induction, triggering increased glutamate release from the presynaptic membrane. Several candidates exist: nitric oxide (NO), carbon monoxide (CO), platelet-activated factor (PAF), arachidonic acid (AA) and BDNF. NO is currently the best candidate, whereas AA is perhaps ruled out (Andersen et al., 2007; Medina and Izquierdo, 1995). The roles and necessity of retrograde messengers in LTP are debated. Retrograde signaling may also be involved in the formation of presynaptic LTP/LTD (Castillo, 2012; Peng et al., 2011).

To obtain a stable LTP, consolidation must occur. Consolidation is the term for any event allowing the transition of unstable E-LTP to stable L-LTP.

1.5.3 Late phase LTP

L-LTP requires new gene expression and protein synthesis, perhaps in cooperation with protein degradation (Bramham and Wells, 2007). As mentioned in paragraph 1.5.1, one event triggering LTP is the influx of Ca^{2+} through NMDARs. Ca^{2+} is important in signaling from the LTP-induced spines to the nucleus, although how this is achieved is currently unclear. Ca^{2+} signaling leads to activation of several important second messengers, for example extracellular signal-regulated kinase (ERK), protein kinase A (PKA), and calcium/calmodulin-dependent protein kinase IV (CaMKIV). BDNF binding to tropomyosin-related kinase B (TrkB) receptors, acetylcholine (ACh) binding to muscarinic receptors, and PKC can all activate ERK through the MAPK pathway. ERK, PKA and CaMKIV can in turn activate nuclear transcription factors (Figure 1.5). One example is the cAMP response-element binding protein (CREB). CREB binds to cAMP response elements (CREs) found in the promoter region of many eukaryotic genes, thereby enhancing gene transcription. CREB targets several immediate early genes (IEGs), such as the transcription factors zif268 and c-fos and Arc/Arg3.1 (activity-regulated cytoskeleton-associated protein / activity-regulated gene 3.1). IEGs are rapidly transcribed in response to neuronal activity (Andersen et al., 2007; Bramham et al., 2010; Peng et al., 2011).

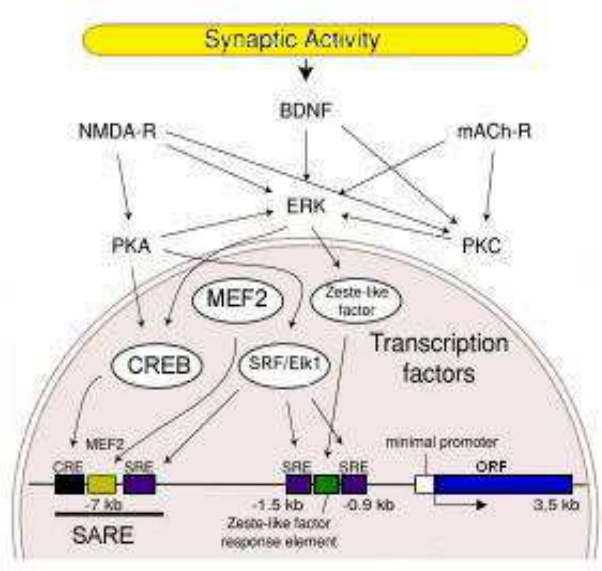

Figure 1.5 | Activity-dependent transcription. Synaptic actrivity leads to activation of kinases, which in turn can activate transcription factors. BDNF, brain-derived neurotrophic factor; CREB, CRE-binding element; CRE, cAMP response element; ERK, extracellular signal-regulated kinase; MEF2, myocyte enhancing factor 2; NMDA-R, NMDA-receptor; ORF, open reading frame; PKA, cAMP-dependent protein kinase; PKC, protein kinase C; SARE, synaptic activity response element; SRE, serum response element; SRF, serum response factor; UTR, untranslated region (Figure modified from Bramham et al., 2010).

The Arc protein is involved in regulation of actin dynamics and homeostatic regulation of AMPAR. Arc is especially intriguing because its messenger RNA (mRNA) is rapidly transported from granule cell somata in the dentate gyrus, selectively into dendrites that have been activated by HFS. Messenger ribonucleoprotein particles (mRNPs) are key protein complexes involved in this mRNA transport and localization. It has been shown that Arc is locally translated at the activated dendritic site, contradicting the obsolete hypothesis that all neuronal protein synthesis happens in the cell body (Bramham et al., 2010; Steward et al., 1998).

The neurotrophin, BDNF, is a trigger for protein synthesis-dependent L-LTP at glutamatergic synapses (Bramham and Messaoudi, 2005). Spine enlargement in CA1 neurons is dependent on protein synthesis and BDNF (Tanaka et al., 2008). HFS of presynaptic neurons triggers BDNF release into the synapse, which activates TrkB receptors, leading to mobilization of further BDNF secretion. BDNF signaling activates Arc-dependent LTP consolidation, and phosphorylation of the actin depolarization factor (ADF/cofilin) in dendritic spines. Blockage of TrkB activation hinders the formation of protein synthesis-dependent L-LTP (Bramham et al., 2008).

1.6 Local protein synthesis

Ribosomes, translation factors and mRNAs have been found in mature dendrites, even in proximity to post-synaptic sites, supporting the idea of *local dendritic protein synthesis* (Bramham and Wells, 2007; Steward and Schuman, 2001; Sutton and Schuman, 2006). A few

proteins synthesized in dendrites are the cytoskeletal proteins Arc and microtubule-associated protein 1B (MAP1B), the α-subunit of the kinase CaMKII (αCaMKII), and the scaffolding molecule postsynaptic density protein 95 (PSD-95) (Grossman et al., 2006; Zalfa et al., 2003). There is evidence implicating local dendritic protein synthesis in synaptic remodeling (Bramham and Wells, 2007; Bramham et al., 2008; Sutton and Schuman, 2006; Tanaka et al., 2008). Change in synaptic structure is bidirectional, and accompanies different forms of synaptic plasticity, such as LTP (Bramham et al., 2010; Tada and Sheng, 2006). LTP consolidation requires actin polymerization, an event associated with enlargement of the postsynaptic density, and spine growth (Figure 1.6) (Bramham and Wells, 2007).

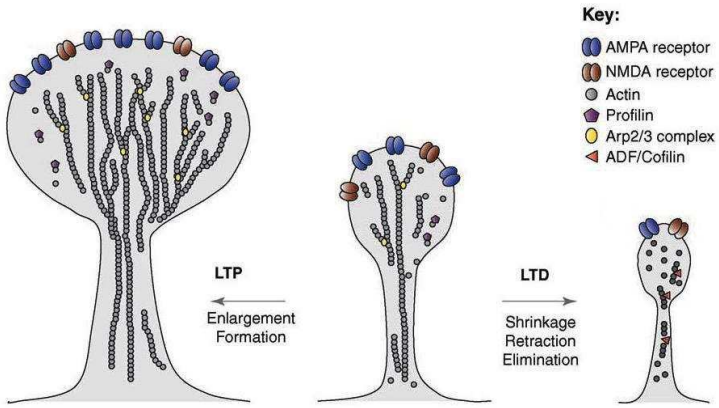

Figure 1.6 | Actin polymerization and spine morphology. In the event of LTP, G-actin monomers polymerize into F-actin chains, leading to spine growth, and more AMPAR are recruited to the postsynaptic membrane. Conversely, during LTD, actin chains depolymerize, resulting in shrinkage or loss of spines (Figure modified from Tada and Sheng, 2006).

Rapid changes in local protein expression occur during changes in synaptic strength. Control of gene expression *at the level of translation* is essential because it allows a rapid, localized control of protein expression. Translation can be controlled by regulation of general transcription factors, which leads to changes in global translation rates, or by mRNA-specific repressors, which permits modulation of local protein composition (Besse and Ephrussi, 2008). MicroRNAs (miRNAs) are diverse, target specific, and their regulation may be reversible, altogether making them attractive candidates for local mRNA-specific translational control.

1.7 MicroRNAs

Only 2-3% of the genome codes for proteins, but 90-95% of the genome is transcribed, suggesting that non-coding RNAs may have important functions, although mostly unknown to this day (Costa, 2010). One important class of non-coding RNAs is miRNAs (Grosshans and Filipowicz, 2008). The first two known miRNAs are lin-4 and let-7. They were both discovered in developmental studies of the nematode *Caenorhabditiis elegans* (Lee et al.,

1993; Reinhart et al., 2000). miRNAs are 20-25 nucleotides in length and major regulators of post-transcriptional gene expression. miRNAs most commonly bind to the 3'untranslated region (UTR) of target mRNAs in a sequence-specific manner, where they act to inhibit translation (Wibrand et al., 2010). miRNAs are primarily found in multicellular organisms, but have been identified in a unicellular alga, *Chlamydomonas reinhardtii*, indicating an evolutionary old origin (Molnar et al., 2007). Hundreds of different miRNAs have been identified in plants and animals, and the number is rapidly increasing. In 2004, the miRBase* only listed 506 miRNA entries from 6 organisms (Griffiths-Jones, 2004), whereas the 18th release of the database from November 2011 contains an astonishing 21643 mature miRNA products from 168 species. The number of miRNAs per organism varies from a handful to up to several hundreds in mammals, and a large proportion of the transcriptome is probably subject to miRNA-mediated translational regulation (Huntzinger and Izaurralde, 2011).

The canonical biogenesis pathway of miRNAs in mammalian cells (Figure 1.7) starts with gene transcription by RNA polymerase II, producing primary miRNA transcripts (pri-miRNAs). Pri-miRNAs form stem-loop structures, with the mature miRNA contained in an imperfectly base-paired double strand stem, joined by a short terminal loop. The RNA-binding protein *Di George Syndrome critical region gene 8* (DGCR8) and the RNaseIII enzyme Drosha are core components of a multiprotein complex processing pri-miRNAs in the nucleus (Treiber et al., 2012). DGCR8 binds to the base of pri-miRNAs, guiding Drosha to cleave pri-miRNAs at their base (cropping step), generating ~70 nucleotides long hairpin structures called miRNA precursors (pre-miRNAs) (Krol et al., 2010). The nuclear export receptor Exportin 5 recognizes pre-miRNAs and mediates their export to the cytosol. In the cytosol, the RNaseIII enzyme Dicer cleaves pre-miRNAs (dicing step), resulting in ~22 nucleotides long double-stranded RNAs (Treiber et al., 2012). In the dicing step, Dicer interacts with transactivation-responsive RNA binding protein (TRBP) and PKR activator (PACT), which both have double-stranded RNA binding domains (Kawahara et al., 2012). Depending on the thermodynamic properties of the two RNA strands, one of them is loaded into an Argonaute protein (Ago) and is incorporated in a multiprotein complex known as the miRNA-induced silencing complex (miRISC) (loading step), whereas the other strand is degraded (Schratt, 2009; Treiber et al., 2012). The core components of the RISC are the proteins Ago and GW182 (glycine-tryptophan protein of 182 kDa), but otherwise little is known about the total RISC protein composition (Krol et al., 2010). The miRISC mediates

* www.mirbase.org

inhibition of protein expression. Loading of miRNA duplexes to Ago proteins is assisted by Hsp70 (heat shock protein of 70 kDa) and Hsp90 (heat shock protein of 90 kDa) chaperones. A miRNA loading complex (miRLC) composed of Dicer, miRNA-free Ago, Hsp90, and TRBP has been identified (Liu et al., 2012). These authors also propose the existence of a miRNA precursor deposit complex (miPDC), whose core is composed of a pre-miRNA directly binding to Argonaute 2 (Ago2). The miPDC is thought to enhance the expression of certain Dicer-dependent miRNAs and to play a crucial role in the maturation of the Dicer-independent miR-451.

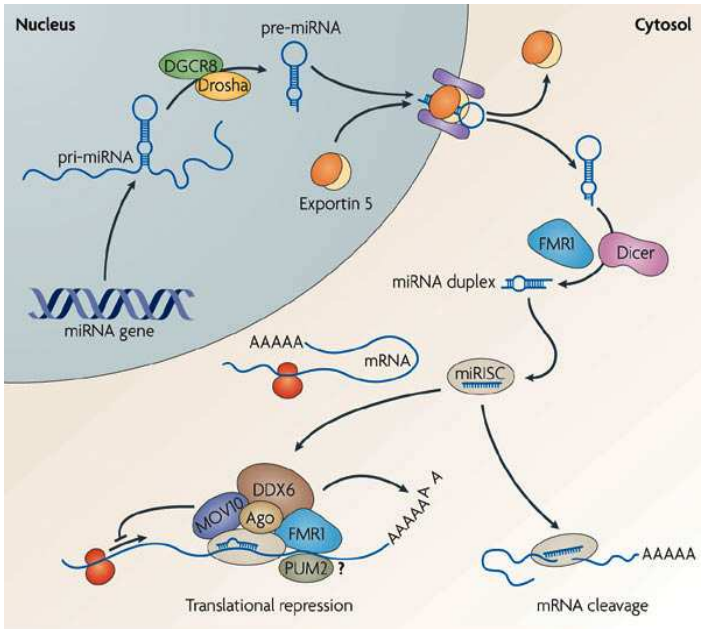

Figure 1.7 | Canonical miRNA biogenesis and mode of action. miRNAs are transcribed as part of primary miRNAs (pri-miRNAs), which are cleaved by Drosha, producing miRNA precursors (pre-miRNA). Pre-miRNAs are exported to the cytosol and further processed by Dicer. One strand from the resulting miRNA duplex is loaded into the microRNA-induced silencing complex (miRISC). The miRISC can bind to target mRNAs by perfect or imperfect base-paring, resulting in degradation or translational repression, by mechanisms still debated (Figure from Schratt, 2009).

1.8 Mechanisms of miRNA-guided post-transcriptional regulation

Translation in dendrites is regulated by postsynaptic glutamate and TrkB receptor signaling (Bramham and Wells, 2007). The miRISC binds to target mRNAs by perfect or imperfect base-paring, usually within the mRNA's 3'UTR (Huntzinger and Izaurralde, 2011; Schratt, 2009). In case of perfect complementarity between the miRNA and mRNA strands, the mRNA undergoes endonucleolytic cleavage, whereas if the complementarity is imperfect, translation of the target is repressed (Krol et al., 2010). Mechanisms of translational repression and mRNA degradation are debated issues (Huntzinger and Izaurralde, 2011).

1.8.1 Translational repression

Protein synthesis can be divided into three steps: initiation, elongation and termination. Translational repression is likely to occur predominantly at the initiation stage of translation (Huntzinger and Izaurralde, 2011). mRNAs possess a 5' cap structure and a 3'-poly(A) tail. The highly conserved poly(A)-binding protein (PABP) interacts with the cap-binding complex eukaryotic translation initiation factor 4F (eIF4F, comprising eIF4E, eIF4G and eIF4A), giving rise to circular mRNAs efficiently translated and protected from degradation. The protein GW182, a protein of the miRNA silencing machinery, interferes with PABP function in translation and mRNA stabilization, perhaps by hindering PABP-eIF4G interaction, or by reducing PABP affinity for the poly(A) tail (Figure 1.8). Both mechanisms interfere with mRNA circularization, and render the 5'cap or poly(A) tail more accessible to mRNA decay enzymes (Tritschler et al., 2010). Surprisingly, some studies have shown that mRNAs lacking a poly(A) tail can be translationally silenced by miRNAs (Ender and Meister, 2010). PABP may even be dispensable for deadenylation and translational repression by the Ago1-RISC in flies (Fukaya and Tomari, 2011). A second model for miRNA-mediated gene silencing is that the miRISC affects eIF4E-cap recognition. A third model proposes that the miRISC blocks association of the 40S and 60S ribosomal subunits. Models for post-initiation translational repression suggest miRISC-mediated ribosome drop-off, or facilitated degradation of nascent peptides. All these hypotheses have been challenged, and more research is necessary to understand which of these mechanisms is/are correct (Carthew and Sontheimer, 2009; Li and Rana, 2012).

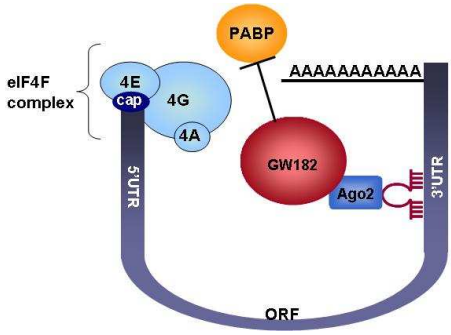

Figure 1.8 | miRNA-mediated translational repression. In this model, proteins of the miRISC interfere with the function of the eIF4F complex and PABP, thereby disabling circularization and subsequent translation of the mRNA. ORF, open reading frame; PABP, poly(A)-binding protein; UTR, untranslated region.

1.8.2 RNA degradation

mRNA degradation is perhaps the predominant mode of mRNA-regulation, at least in cultured mammalian cells. It is not known whether degradation is a consequence of translational inhibition. Degradation involves the recruitment of deadenylase complexes to mRNAs. The protein GW182 is known to interact with the two deadenylase complexes PAN2-PAN3 and CCR4-NOT, which deadenylate the target mRNAs, disabling circularization via PABP, silencing the mRNAs for translation (Figure 1.9). Surprisingly, deadenylation has been reported to occur both before and after translational repression, and even at untranslated mRNAs, indicating translation-independent degradation (Huntzinger and Izaurralde, 2011; Treiber et al., 2012). After deadenylation, target mRNAs are decapped by the enzyme mRNA decapping enzyme 2 (DCP2) and subsequently degraded by a 5'→3' exoribonuclease, XRN1, or degraded by 3'→5' decay by the exosome complex. The degradation is thought to take place in processing bodies (P-bodies). P-bodies are eukaryotic cellular structures enriched in mRNA-catabolizing enzymes and translational repressors (Eulalio et al., 2007; Filipowicz et al., 2008). miRNAs are important for regulation of gene expression, therefore miRNA levels and function have to be tightly controlled.

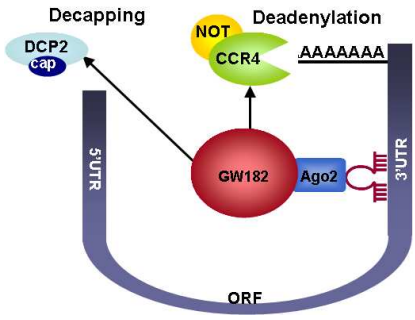

Figure 1.9 | miRNA-mediated mRNA degradation. Target mRNAs are deadenylated by recruited deadenylase complexes such as CCR4-NOT or PAN2-PAN3 (not shown), followed by decapping by the enzyme DCP2. The mRNA is degraded by XRN1-mediated 5'→3' decay, or exosome-mediated 3'→5' decay. DCP2, mRNA decapping enzyme 2; ORF, open reading frame; UTR, untranslated region.

1.9 Regulation of miRNA biogenesis and function at the synapse

There are several brain-specific miRNAs, such as miR-134. miRNAs in the brain are involved a range of processes, such as synapse formation and maturation, neurological disorders, neural plasticity and memory. Activity-regulated transcription factors such as CREB can control the expression of miRNAs at the level of transcription. miRNAs and transcription factors frequently form autoregulatory feedback loops. Control of proteins involved in miRNA biogenesis is another mechanism for modulating the pattern of miRNA expression. The NMDAR- and TrkB receptor-activated MAPK/ERK signaling pathway can lead to

stabilization of TRBP, and thus stabilization of its partner, Dicer. Accessory proteins such as Lin-28 can also interact with processing proteins such as Drosha or Dicer (Krol et al., 2010; Schratt, 2009). Editing of precursor miRNAs, for example adenosine base conversion to inosine by adenosine deaminases acting on RNA (ADARs), suppresses miRNA biogenesis at both the cropping and dicing steps (Kawahara et al., 2012). Another way of controlling miRNA-mediated silencing is by regulation of miRISC proteins. The core components of the miRISC, Ago and GW182, as well as other proteins, are probable targets for regulation (Krol et al., 2010).

1.9.1 Argonaute proteins

Argonaute (Ago) proteins are specialized small-RNA-binding proteins, with a molecular mass of ~100 kDa. They bind mature miRNAs directly, and mediate miRNA-guided gene silencing. Ago proteins can be divided into two subfamilies: the Ago subfamily and the Piwi subfamily. Humans express four genes of the Ago subfamily, named Ago1-4. Ago proteins have an ancient origin, and are conserved throughout species. Studies on bacteria and archaea have revealed Ago protein structure, but mammalian Ago structure is still unavailable. All Ago proteins have a PAZ- (PIWI-Argonaute-Zwille), MID- (middle domain) and PIWI-(P-element-induced wimpy testes) domain (Figure 1.10). The PAZ domain binds the 3' end of miRNAs, whereas the MID domain binds their 5' end. The catalytic activity of the miRISC, also called Slicer activity, lies in the Ago protein itself, more specifically within the PIWI domain. In mammals, only Ago2 is endonucleolytically active (Ender and Meister, 2010; Treiber et al., 2012).

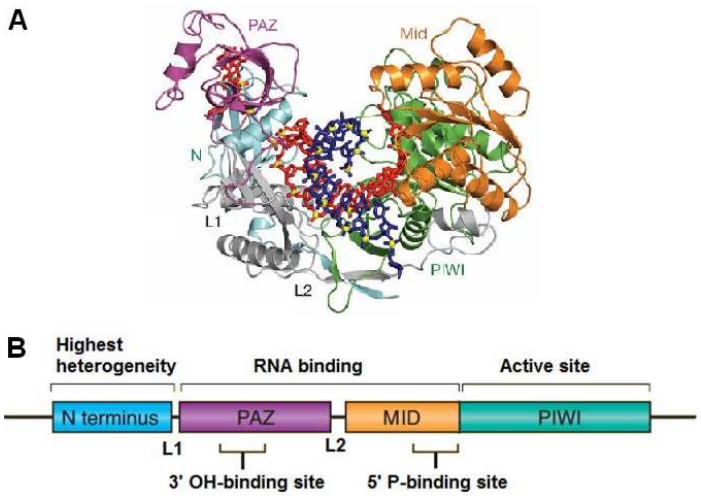

Figure 1.10 | Argonaute protein structure. **(A)** Crystal structure of Argonaute from the bacteria *Thermus thermophilus* (Wang et al., 2008). **(B)** Domain organization of Ago proteins. The PAZ and MID domains bind miRNA, whereas the PIWI domain is the active site for endonucleolytic activity (Ender and Meister, 2010).

Regulation of Ago proteins may take part in regulation of miRNA function. Different Ago proteins may have distinct functions, and differences in the cellular concentration of individual Ago proteins may affect miRISC function. Modifications of Ago proteins may also be important. Polyubiquitylation and subsequent proteasomal degradation leads to impaired miRNA-mediated silencing, and hydroxylation or Ser387 phosphorylation leads to Ago2 stabilization and increased P-body localization (Krol et al., 2010). Tyr529 phosphorylation reduces small-miRNA-binding (Rudel et al., 2011).

1.9.2 GW182 proteins

GW182 proteins interact with Ago, and are required for miRNA-mediated silencing (Tritschler et al., 2010). They are named so because they contain glycine (G) and tryptophan (W) repeats, and have a molecular mass of 182 kDa. Insects have only one GW182 paralog, whereas mammals have three (TNRC6A, TNRC6B and TNRC6C), with multiple splice variants (Krol et al., 2010). A 210 kDa isoform of human GW182 named trinucleotide GW1 (TNGW1) has been reported (Li et al., 2008). Insects and vertebrates share a conserved central ubiquitin associated-like domain (UBA) and a C-terminal RNA recognition motif (RRM) (Figure 1.11). Despite conservation, those domains are not strictly required for GW182 silencing activity. The N-terminal GW repeat-containing region binds Ago proteins, whereas the C-terminal- and M-GW repeats-containing regions promote translational repression and degradation of miRNA targets. Intriguingly, those regions are not highly conserved, and the number of GW repeats varies for different GW182 proteins (Tritschler et al., 2010).

The exact mechanism by which GW182 proteins contribute to silencing is not perfectly understood, but some GW182 interactions are known. GW182 interacts with poly(A)-binding protein 1 (PABP1) and interferes with PABP1 function in translation and mRNA stabilization (Figure 1.8). GW182 proteins also interact with the two deadenylase complexes PAN2-PAN3 and CCR4-NOT (Figure 1.9). The GW182 interactions with PABP1 and the deadenylase complexes are conserved throughout evolution, meaning that these interactions are probably important for miRNA-mediated gene silencing (Kuzuoglu-Ozturk et al., 2012).

GW182 proteins accumulate in P-bodies, yet these are not required for mRNA silencing and degradation, suggesting that this localization may be a consequence of silencing (Eulalio et al., 2009; Tritschler et al., 2010). Little is known about the regulation of GW182

proteins. TNRC6A is highly phosphorylated, although the significance of this phosphorylation is unknown (Krol et al., 2010). TNRC6A may also undergo ubiquitylation.

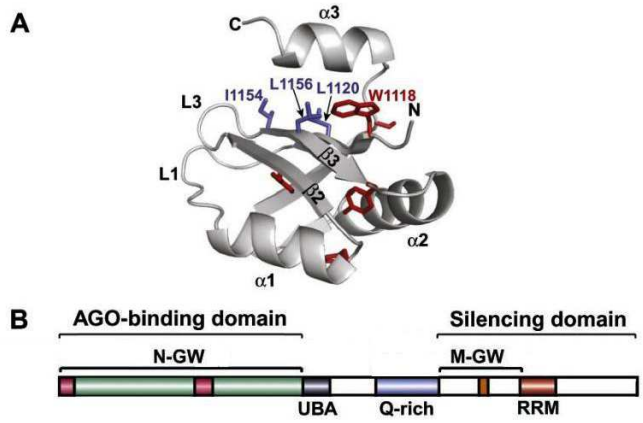

Figure 1.11 | Dm GW182 protein structure. (A) Ribbon diagram of *Drosophila melanogaster* (Dm) GW182 structure. **(B)** Domain organization of Dm GW182. N-GW, N-terminal glycine and tryptophan (GW) repeats; M-GW, middle GW repeats; UBA, ubiquitin associated-like domain; Q-rich, region rich in glutamine (Q); RRM, RNA recognition motif (Figure modified from Eulalio et al., 2009).

1.9.3 Other RISC proteins

The miRISC contains many proteins other than Ago and GW182, required for miRNA function or modulation. DDX6, MOV10, Dicer and FMRP are proteins thought to be associated with Ago2 and perhaps part of the RISC.

DEAD (Asp-Glu-Ala-Asp) box polypeptide 6 (DDX6), also known as RCK/p54 in humans, is an evolutionary conserved 54 kDa ATP-dependent RNA helicase, localized to P-bodies and stress granules. DDX6 interacts with Ago1 and Ago2 in P-bodies of human cells, and is required for miRNA-induced gene silencing (Chu and Rana, 2006). Surprisingly, overexpressed DDX6 in cultured neuronal cells interacts with amyloid precursor protein (APP) mRNA as part of a multi-protein complex and results in elevated levels of APP mRNA and protein (Broytman et al., 2009). DDX6 is required for efficient replication of hepatitis C virus (HPC) replication, suggesting a role for DDX6 in HCV genome amplification and/or maintenance of cellular homeostasis (Jangra et al., 2010). DDX6 cooperates with the zing finger homolog tristetraprolin (TTP) in AU-rich element (ARE)-dependent translational repression (Qi et al., 2012). Taken together, these studies suggest that the helicase DDX6 may have a role in balancing activation and repression of translation (Minshall et al., 2009).

Moloney leukemia virus 10 protein (MOV10) is a 114 kDa RNA helicase required for miRNA-mediated mRNA cleavage. It is a homologue of the Drosophila DExD/H-box RNA helicase Armitage. MOV10 binds Ago1 and Ago2 to mediate miRNA-induced translational repression (Meister et al., 2005). MOV10 is present at synapses and NMDAR-mediated synaptic activity promotes MOV10 degradation by the proteasome. MOV10 may be

dissociated from the RISC and degraded as a result of NMDAR-mediated synaptic activity, relieving miRISC-mediated translational repression (Banerjee et al., 2009). Overexpressed MOV10 is able to reduce the infectivity of human immunodeficiency virus type 1 (HIV-1) by inhibiting replication, whereas reduced MOV10 expression increases HIV-1 infectivity (Wang et al., 2010).

Dicer is a 215kDa RNase III enzyme involved in the cleavage of pre-miRNA in the canonical miRNA biogenesis pathway. Dicer excises miRNAs from the stems of stem-loop pre-miRNAs to generate double-stranded miRNA duplexes. One of the strands is loaded onto Ago2, forming the minimal miRISC. Dicer is part of the miRNA loading complex, composed of Dicer, miRNA-free Ago, Hsp90, and TRBP. Mammals have only one Dicer protein, whereas other organisms may have several, for example the fly *Drosophila Melanogaster* expresses two Dicers (Carthew and Sontheimer, 2009). A well-studied mechanism for regulation of Dicer processing of pre-miRNAs is regulation by the protein Lin-28. Lin-28 binds to the terminal loop of most let-7-family miRNAs, and Lin-28 recruits a specific uridyl transferase (TUTase), TUT4. TUT4 in turn polyuridylates the let-7 pre-miRNA targeted by Dicer at its 3'end, thereby repressing Dicer function. This mechanism is highly conserved throughout evolution (Treiber et al., 2012). There is competition between Dicer mRNA and pre-miRNAs for export from the nucleus through Exportin 5, and Dicer is downregulated by overexpression of pre-miRNAs in human cells (Bennasser et al., 2011).

Fragile-X mental retardation protein (FMRP, also called FMR1) is a highly conserved, 70-80 kDa RNA-binding protein, highly expressed in the brain and testes. The absence of FMRP causes fragile-X syndrome, the most common form of inherited mental retardation (Bagni and Greenough, 2005; Bassell and Warren, 2008). FMRP is localized to dendrites and synapses, and is thought to function as a translational repressor of specific mRNAs, including the dendritically translated mRNAs MAP1B, α-CaMKII, PSD-95 and Arc, all involved in synaptic plasticity (Bassell and Warren, 2008; Edbauer et al., 2010). FMRP-mediated translational repression may function through a ribonucleoprotein complex that contains the small dendritic non-translatable RNA *BC1*. *BC1* may recruit FMRP to its target mRNAs (Zalfa et al., 2003). FMRP selectively binds ~4% of the mRNA in the mammalian brain, and is associated with actively translating polyribosomes in cultured neurons and brain synaptoneurosomes. FMRP may act as a regulator of translation as a response to group I mGluR activation, contributing to mGluR-LTD. Several studies indicate that FMRP function may be controlled by phosphorylation (Muddashetty et al., 2011; Narayanan et al., 2008). It is also possible that FMRP plays a role in mRNA stability and transport (Bassell and Warren,

2008; Muddashetty et al., 2011). FMRP interacts with RISC proteins such as Ago2 and Dicer, and associates with miRNAs, but is not essential for RNAi-mediated mRNA cleavage (Edbauer et al., 2010). FMRP may not influence RISC function, but rather play a role in stress granule formation (Didiot et al., 2009).

1.10 Project goals and methodological approach

Neuronal plasticity requires both rapid *de novo* protein synthesis and protein degradation. Regulation of translation occurs mainly at the initiation step, for example through phosphorylation of initiation factors. In LTP, the critical time period for protein synthesis in most synapses lasts less than one hour, meaning the regulation of protein synthesis must be rapid. Alteration of mRNA stability is a rapid mechanism for the control of protein synthesis, and miRNAs have emerged as key regulatory molecules of mRNA stability. miRNAs bind complementarily to their target mRNAs and recruit a specific set of proteins, forming the miRISC. The miRISC can interfere with PABP and hinder circularization of the mRNA, thereby hindering translation. The miRISC can also promote degradation of the mRNA by recruiting deadenylase complexes and decapping enzymes. However, little is known about the regulation of miRNA function in the brain.

Here, we examine how miRNA function is regulated during synaptic plasticity, by determining whether the protein composition of the miRISC changes after induction of LTP in the mammalian brain. The study is a collaboration with a former PhD student in our lab, Balagopal Pai. To our knowledge, we are the first to study the protein composition of the miRISC during LTP. LTP was induced at the perforant path in the dentate gyrus of anaesthetized rats. Monoclonal Ago2 antibodies were used to co-immunoprecipitate Ago2-associated proteins from the dentate gyrus lysate. Five proteins thought to bind the core component of the miRISC, Ago2, were analyzed by Western blotting. These proteins were GW182, the RNase III enzyme Dicer, the RNA-binding protein FMRP, and the RNA helicases MOV10 and DDX6. The time points chosen for analysis of miRISC modulation were 30 minutes and 2 hours after the induction of LTP. These time points correspond to two stages of LTP, at which protein expression in the induced spines may be different. In addition, mass spectrometry was used to identify potentially new protein constituents of the brain miRISC.

Project goals

Goal 1

Use immunoprecipitation (IP) to investigate whether the proteins GW182, Dicer, FMRP, MOV10 and DDX6 are associated with Ago2 in the rat dentate gyrus *in vivo*, and whether these associations are modulated during LTP.

Goal 2

Use mass spectrometry to identify new candidate Ago2 binding partners and to investigate whether these proteins are modulated during LTP.

2 Materials and methods

2.1 Electrophysiology and microdissection

Electrophysiology and microdissection were performed by Birgitte Berentsen. Experiments followed the established protocols from the Bramham Lab. Animal experiments were conducted in accordance with the European Community Council Directive of November 24th, 1986 and approved by the Norwegian Committee for Animal Research.

Male Sprague-Dawley rats weighing at least 250 g were used. The rats were anaesthetized by intraperitoneal injection of urethane (1.5 mg/kg), and placed in a stereotaxic apparatus. A stimulating electrode was inserted in the left brain hemisphere at specific stereotaxic coordinates, to stimulate the medial perforant path. A recording electrode was inserted ipsilaterally in the hilar region of dentate gyrus, at the depth where the recorded positive-going field excitatory-post-synaptic-potential (fEPSP) reached its maximal slope. The contralateral (right) hemisphere served as a control. Test pulses were applied to the perforant path at 0.033 Hz throughout the experiment, except during HFS. The baseline response was recorded for 20 min. The pattern for induction of LTP by HFS consisted of eight pulses at 400 Hz, repeated four times at 10 seconds interval. This HFS-session was repeated twice, at 5 min interval. Signals from the hilus were amplified, filtered, and digitized. After HFS, induced responses were recorded for 30 min or 2 hrs, and the rats were immediately decapitated. The hippocampus of each brain hemisphere was rapidly microdissected from the cortex, followed by separation of the dentate gyrus and hippocampus proper. The tissues were flash frozen in a mixture of 96%* methanol and dry ice, before storage at -80ºC.

The fEPSP was analyzed with the software DataWave Experimental WorkBench (DataWave Technologies, Longmont, CO, USA). An analysis of variance (ANOVA) was performed, based on the values of the last 5 min of baseline. Details on surgery and electrophysiology have previously been described (Messaoudi et al., 2002; Panja et al., 2009).

* All percentages in this chapter are volume / volume percentages.

2.2 Antibodies

Anti-EIF2C2 (Ago2) antibody from Abnova was used for IP and Western blotting (monoclonal mouse, dilution 1:1000). Other antibodies used for Western blotting were: anti-β-actin (cytoskeletal) from Bethyl laboratories (polyclonal rabbit, 1:1000), anti-Arc (C7) from Santa Cruz Biotechnology (monoclonal mouse, 1:200), anti-DDX6 from Bethyl laboratories (polyclonal rabbit, 1:500), anti-Dicer, a gift from Prof. W. Filipowicz at the Friedrich Miescher Institute in Switzerland (polyclonal rabbit, 1:1000), anti-FMRP from Abcam (polyclonal rabbit, 1:1000), anti-GW182 (H70) from Santa Cruz Biotechnology (polyclonal rabbit, 1:20), anti-GW182 from Bethyl laboratories (polyclonal rabbit, 1:1000), and anti-MOV10 from ProteinTech Group (polyclonal rabbit, 1:250). Primary antibodies were diluted in 5% bovine serum albumine (BSA). Secondary antibodies used were: Horseradish Peroxidase (HRP) conjugated goat anti-mouse (1:2000) from Calbiochem and Millipore, and HRP-conjugated goat anti-rabbit (1:2000) from Calbiochem. Secondary antibodies were diluted in 1× Tris-buffered saline (TBS) supplemented with 0.1% Tween20 (1×TBST).

2.3 Cell culture and transfection

Human embryonic kidney (HEK) 293T cells were grown in Dulbecco's Modified Eagle's Medium (DMEM, Sigma Aldrich), supplemented with 10% fetal bovine serum (Sigma Aldrich/Gigco) and 8 mM L-glutamine at 37ºC and 5% CO_2. The cells were grown to 90-95% confluence (~24 hrs), and transfected with plasmids expressing Ago2 fused to enhanced green fluorescent protein, (EGFP-Ago2 was a gift from Prof. Philip Sharp's lab at MIT, MA, USA), using the 6-well protocol for Lipofectamine™ 2000 (Invitrogen, see appendix for link to user manual). Lipofectamine is a cationic lipid, binding the negatively charged DNA and mediating fusion of the transfection complex with the cell membrane. Less than 24 hrs after transfection, the cells were harvested and lysed in lysis buffer containing 5 µl of 0.1% Triton (X100, SigmaUltra, Sigma Aldrich), 50 µl phenylmethylsulfonyl fluoride (PMSF, Sigma Aldrich), and ½ tablet of protease inhibitor (Complete, Mini, Protease Inhibitor Cocktail Tablets, Roche), in 5 ml of 1×PBS. The lysates were clarified by centrifugation at 10 000 rpm for 20 min at 4ºC.

2.4 Tissue homogenization and protein determination

Dentate gyrus tissues were individually hand-homogenized with 8 strokes in 300 µl of freshly made lysis buffer on ice, containing 20 mM Tris-HCl, 150 mM NaCl, 2 mM $MgCl_2$, 0.5 mM DTT, 1 mM NaF, 2 mM EDTA, 0.5% NP40, RNase inhibitor (1 µl/sample, Riobolock™ RNase Inhibitor, Fermentas), and protease inhibitor (1 tablet/10 ml, Complete, Mini, Protease Inhibitor Cocktail Tablets, Roche). The homogenates were centrifuged at 10 000 rpm for 20 min at 4ºC and the pellets were discarded. Protein concentrations in the dentate gyrus homogenates and the EGFP-Ago2-transfected HEK cells were determined by using the microplate procedure of the Thermo Scientific Pierce® BCA Protein Assay Kit (see appendix for link to user manual). 10 µl of diluted sample (1:10) was loaded into three replicate wells, together with 190 µl of working reagent*, and incubated for 30 min at 37ºC on a gyro rocker. Bovine serum albumine (BSA) was used as a standard.

The bicinchoninic acid (BCA) assay combines the reduction of copper(II) ions (Cu^{2+}) to copper(I) ions (Cu^{+}) by protein peptide bonds in an alkaline solution (Biuret reaction), and the chelation of two BCA molecules with one Cu^{+}, forming a purple-colored product exhibiting strong absorbance at 562 nm (Smith et al., 1985). This assay was chosen because it is compatible with the detergents in the lysis buffer.

2.5 Co-immunoprecipitation

Immunoprecipitation (IP) is a type of affinity chromatography, used for purification of a protein. The protein is precipitated out of a solution by using an antibody coupled to a solid substrate (Protein A/G-conjugated agarose beads) against the antigen of interest. Co-immunoprecipitation (co-IP) is a technique for the analysis of protein-protein interactions, in which any protein bound to the selected antigen will be precipitated together with it.

Protein G Sepharose beads (45 µl/sample, GE Healthcare) were washed 4 times in 500 µl of 1× phosphate buffered saline (PBS), and centrifuged at 3000 rpm for 3 min at 4°C between each wash. Ago2 antibody (3 µg/sample) was added to the beads diluted in 1×PBS (100 µl/sample). Ago2 antibody and beads were incubated on a rotator either for 1 hr at room temperature (RT), or preferably overnight at 4°C. After incubation, the antibody-bound beads were washed 1-2 times with 500 µl of 1×PBS, and divided equally between as many tubes as there were samples. For each sample, 750 µg of protein was added to the antibody-bound

* Working reagent is provided in the Pierce® BCA Protein Assay Kit.

beads diluted in 400 µl of lysis buffer, and incubated on a rotator for 3 hrs at 4°C. The protein-antibody-bead complex was collected by centrifugation. Nonspecifically bound proteins were removed by washing the beads 3 times with 500 µl of lysis buffer, with 3 min of centrifugation at 3000 rpm at 4°C between each wash. The immunoprecipitated complex was eluted from the beads, denatured and reduced by adding 30 µl of 2× sample buffer (XT sample buffer, BioRad), and boiled at 95°C for 5 min. 40 µl of unbound proteins from each IP were denatured in 10 µl of 4× sample buffer. For each sample, 75 µg of total homogenate was denatured in 2× sample buffer. Ago2 immunoprecipitated from EGFP-Ago2-transfected HEK cells was used as a positive control for the experiment, whereas antibody-bound beads alone were used as a negative control.

2.6 SDS-PAGE

Sodium dodecyl sulphate polyacrylamide gel electrophoresis (SDS-PAGE) is a method for separating proteins according to their size. Protein samples are denatured and reduced by a sample buffer, and then separated in a polyacrylamide gel composed of an upper stacking gel and a lower resolving gel. An electric field is applied across the gel, causing the reduced proteins to migrate toward the anode (+) through the pores of the gel, in a speed reversely proportional to size.

Immunoprecipitated samples, total homogenates and unbound proteins (from IP) were separated by SDS-PAGE in a 1.5 mm thick polyacrylamide gel (see appendix), alongside protein standard (Precision Plus Protein Dual Color Standards, BioRad). The proteins were concentrated in the stacking gel at 80 V, and then separated in the resolving gel for 2-3 hrs at 100 V in a Mini-PROTEAN® 3 Cell (BioRad, see appendix for link to user manual).

2.7 Western blotting

Western blotting is a method used to detect proteins present in a sample. After separation of the proteins by SDS-PAGE, the proteins are transferred from the gel to a protein-binding membrane by electrophoretic transfer, and subsequently detected by enzyme-conjugated antibodies. An appropriate substrate is added to produce a detectable product, such as chemiluminescence or fluorescence.

The proteins were transferred to a nitrocellulose membrane (Amersham Hybond ECL Nitrocellulose Membrane, GE Healthcare) by electrophoretic transfer, either at 100 V for 1.5

hrs at RT, or 21 V overnight at 4°C, in a Mini Trans-Blot® Electrophoretic Transfer Cell (BioRad, see appendix for link to user manual). Membranes were stained with Ponceau S dye and cut into several bands. The Ponceau S dye was rinsed off with ddH_2O and 1×TBST. Then the membranes were blocked with 5% non-fat dry milk in 1×TBST for 1 hr at RT on a gyro rocker. After blocking, the membranes were incubated in primary antibody on a gyro rocker for either 2 hrs at RT, or preferably overnight at 4°C. After washing 3×5 min with 1×TBST, the membranes were incubated in secondary antibodies for 1 hr at RT, and washed again 3×7 min with 1×TBST. The selected secondary antibodies were coupled to the enzyme horseradish peroxidase, allowing detection of the protein bands by the use of a chemiluminescent substrate for the enzyme (Thermo Scientific Pierce® ECL Western Blotting Substrate, see appendix for link to user manual). To re-probe the membrane with different antibodies, the membrane could be washed 3×5 min with 1×TBST, stripped with mild stripping buffer (15 g/l glycine, 1 g/l SDS, 1% Tween20, pH 2.2) for 1hr, and washed 3×5 min with 1×TBST. Chemiluminescence was detected by a Gel Documentation System. Band intensities were quantified using the software Quantity One (Bio-Rad). Student's t-test for dependent samples was used for statistical analysis of the difference between LTP-induced samples and their controls. The p-value for significance was 0.05.

2.8 Mass spectrometry

Mass spectrometry (MS) is an analytical technique used for determining the mass of particles in a sample, from which peptide and protein composition can be elucidated. Proteins excised from an SDS-PAGE gel are reduced and alkylated to increase the accessibility for trypsin digestion, which leads to specific cleavage at arginine (R) and lysine (K) residues (Figure 2.12). Peptides are desalted and concentrated by binding to a matrix, to improve mass spectra quality. MS instruments consist of an ion source, a mass analyzer and a detector. After ionization, the mass analyzer separates the ions according to their mass-to-charge ratio (m/z). The ions are detected and the signal is processed into mass spectra. Tandem mass spectrometry (MS/MS) can be used to predict the identity of proteins. Selected ions from a first round of MS are fragmented, and these fragments undergo a second round of MS.

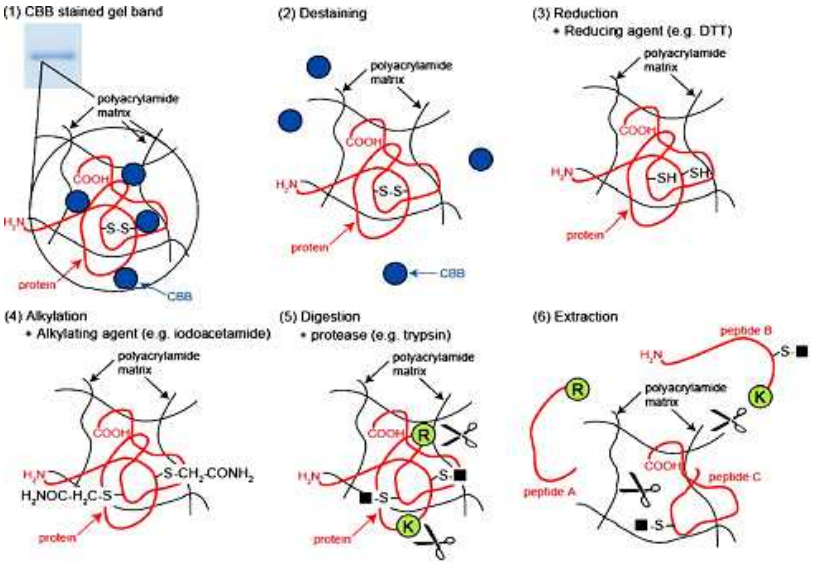

Figure 2.12 In-gel trypsin digestion. (1) Polyacrylamide gel stained with Coomassie Brilliant Blue. (2) Destaining by ABC and ACN. (3) Reduction by DTT and (4) alkylation by IAA to increase digestion efficiency. (5) Protein digestion by trypsin at R and K amino acid residues. (6) Extraction of the peptides (Figure modified from Granvogl et al. 2007).

Immunoprecipitated samples were separated by SDS-PAGE at 80 V in a 0.75 mm thick gel for about 15 min after reaching the resolving gel. The gel was treated in a fixing solution (50% methanol, 10% acetic acid) for 30 min shaking at RT, stained with Coomassie blue dye (50% methanol, 7% acetic acid, 2.5 g/l Coomassie Brilliant Blue) overnight shaking at RT, and destained in destaining solution (50% methanol, 7% acetic acid) overnight shaking at RT. The stained protein-containing bands were excised and cut into 1×1 mm squares, and the dye was removed by alternately incubating the cubes with 100 µl of 50 mM ammonium bicarbonate (ABC) and 100 µl of acetonitrile (ACN), 3×5 min at RT. The cubes were incubated in reduction buffer (6.5 mM DTT in 50 mM ammonium bicarbonate) for 1 hr at 60ºC shaking, shrunk with ACN, and incubated in alkylation buffer (54 mM iodoacetamide in 50 mM ammonium bicarbonate) for 20 min at RT in the dark. Before digestion, the gel cubes were washed with successive incubations of 100 µl of 50 mM ABC and 100 µl of ACN, 2×5 min at RT. After rehydration of the gel cubes in 20 µl of digestion buffer (10 µl trypsin in 140 µl ammonium bicarbonate) for ~30 min, 10-20 µl of ABC was added, and digestion was allowed to proceed overnight (≤16 hrs) at 37°C. After digestion, the supernatant was collected, and peptides were extracted from the gel by incubation in 60 µl of 10% formic acid (FA) for 10 min at RT followed by incubation in 50 µl of ACN for 5 min at RT. The extraction step was repeated once. The peptide solution was concentrated to a volume of ~10 µl by vacuum centrifugation.

A STAGE (Stop And Go Extraction) tip column was prepared by wedging two small pieces of C18 Empore 3M Extraction Disk approximately 3 mm above the narrowest part of a 200 µl pipette tip. The C18-matrix was activated by slowly pushing 20 µl of methanol

through the STAGE tip by means of a syringe, followed by equilibration with 20 µl of buffer B (0.5% acetic acid, 80% acetonitrile) and washing with 20 µl of buffer A (0.5% acetic acid). The peptide sample was loaded and pushed out, leaving the peptides bound to the Empore disk. Washing with buffer A was repeated, and the peptides were eluted by pushing through 10 µl of buffer B, twice. The eluted peptides were collected in Protein LoBind Eppendorf tubes and vacuum centrifuged until ~2 µl remained.

After sample preparation, mass spectrometry itself was conducted by Olav Mjaavatten at The Proteomics Unit at University of Bergen (PROBE), supported by the National Program for Research in Functional Genomics (FUGE) funded by the Norwegian Research Council. The instrument used was an Orbitrap Velos Pro (Thermo Scientific) equipped with a nanospray Flex ion source (Thermo Scientific). The data were matched against the Swissprot protein database using the mascot search engine[*].

[*] http://www.matrixscience.com/

3 Results

3.1 Long-term potentiation was induced by high-frequency stimulation

Fibers of the medial perforant path in the hippocampus form synapses with the granule cells of the dentate gyrus. By stimulating this pathway with a single electrical stimulus-pulse, an electrical potential is generated on the postsynaptic side of the granule cells. This potential is called a field excitatory post-synaptic potential (fEPSP), and can be recorded (Figure 3.1). The recording electrode was placed in the hilar region of the dentate gyrus, and baseline response to test pulses at 0.033 Hz was recorded for 20 min. LTP can be induced at the granule cell synapses by applying HFS to the medial perforant path, using the protocol described in the methods chapter. HFS was applied to the medial perforant path on the left side of the rat brain, whereas the right side was an unstimulated control. The fEPSP response to HFS was recorded for either 30 min or 2 hrs post-HFS. The two chosen time points correspond to different stages of LTP, at which protein expression in the induced spines may be different, and the composition of the miRISC may vary. HFS led to a stable and robust increase of the fEPSP in the hilar region of the dentate gyrus, confirming successful induction of LTP. The average change of fEPSP from baseline was 48 ± 7% (n = 6) for experiments recorded for 30 min post-HFS (Figure 3.2 A), and 29 ± 6% (n = 8) for experiments recorded for 2 hrs post-HFS (Figure 3.2 B). For both time points, the changes were statistically significant ($p < 0.001$). Immediately after the electrophysiological experiments, the dentate gyri were microdissected from the cortex.

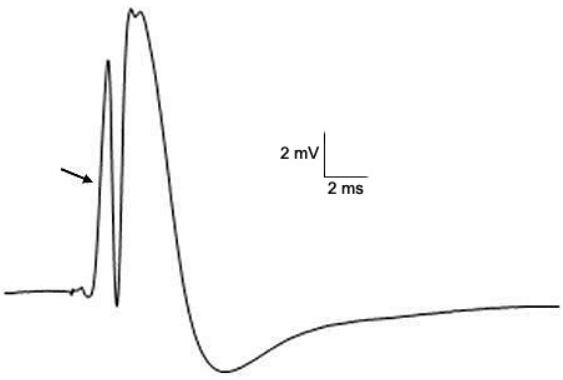

Figure 3.1 | Field excitatory post-synaptic potential (fEPSP). The figure shows a typical fEPSP recording as response to a single test-pulse. The fEPSP slope was determined by calculating the average of five points along the rising segment of the first positive peak (showed by the arrow).

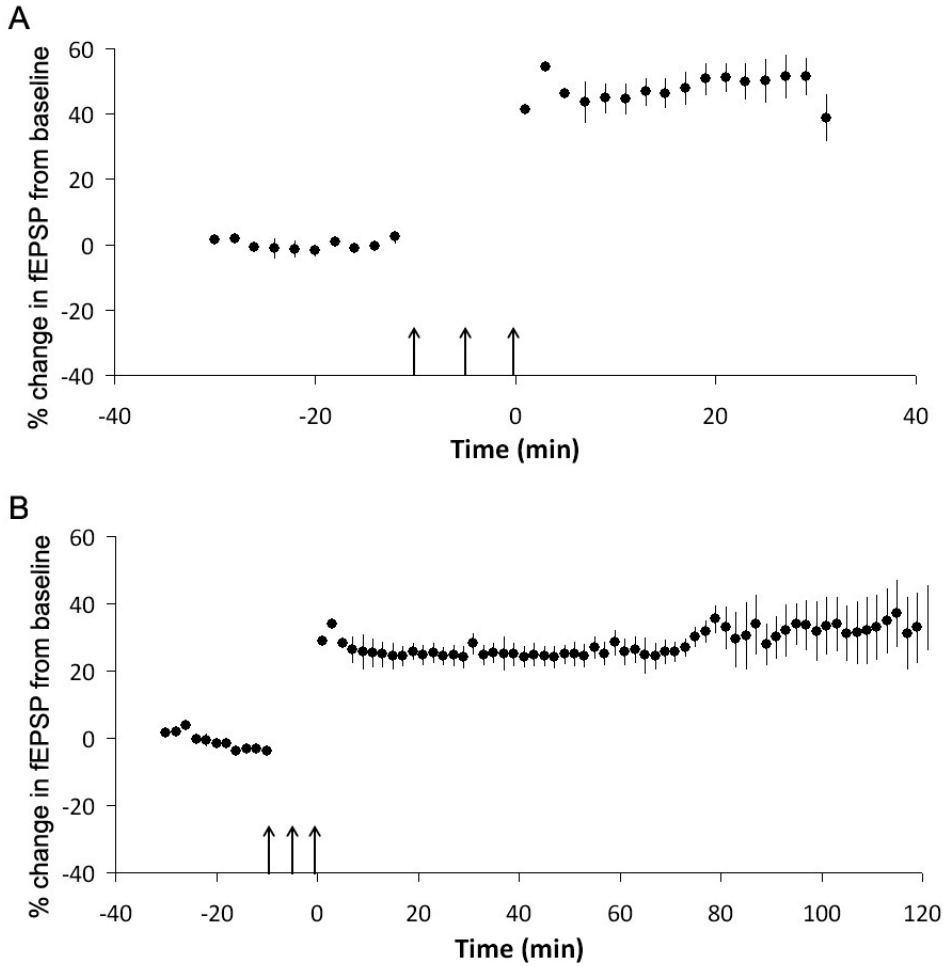

Figure 3.2 | Time course plots for HFS-induced changes in fEPSP. Each point in the chart represents the average fEPSP of the experiments, for 2 min. The baseline is the response to test pulses at 0.033 Hz, recorded for 20 min before HFS. The arrows represent the three sessions of HFS. **(A)** fEPSP recording for 30 min post-HFS. The average increase of the fEPSP was 48 ± 7% ($n = 6$, $p < 0.001$). **(B)** fEPSP recording for 2 hrs post-HFS. The average increase of the fEPSP was 29 ± 6% ($n = 8$, $p < 0.001$). Plots provided by Birgitte Berentsen.

3.2 Western blotting

The dentate gyri were homogenized in lysis buffer, and total protein concentration in lysates was determined using the BCA assay. Western blotting was performed for total lysates. For each sample, 75 µg of protein was loaded onto the SDS-PAGE gel, and equal loading was confirmed by probing the blots for the housekeeping gene β-actin (Figure 3.3).

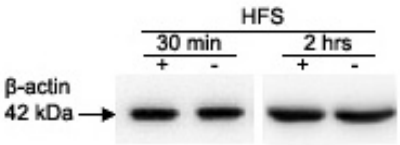

Figure 3.3 | β-actin as a control for equal protein loading. Representative immunoblot showing β-actin in total lysate. β-actin was used as a control for equal protein loading in SDS-PAGE.

3.3 Arc was induced by high-frequency stimulation

The Arc protein is critical for many forms of protein synthesis dependent plasticity. It is involved in regulation of actin dynamics and homeostatic regulation of AMPA receptors. The gene Arc/Arg3.1 is rapidly transcribed in response to neuronal activity. Sustained Arc synthesis is necessary for HFS-induced LTP. Infusion of Arc antisense 2 hrs after HFS leads to a complete reversal of LTP (Messaoudi et al., 2007). Therefore, the immunoblots of total lysate were probed for Arc. The protein was consistently and significantly detected in the dentate gyri stimulated by HFS, both 30 min and 2 hrs post-HFS, and was not expressed in the unstimulated controls (Figure 3.4). As a precaution, dentate gyri that did not express Arc in the HFS-treated side were excluded from this study.

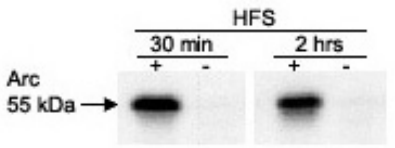

Figure 3.4 | Arc induction by HFS. Representative immunoblot showing Arc in total lysate. Both 30 min and 2 hrs post-HFS, Arc protein expression was induced in HFS-treated dentate gyri (+), but not in unstimulated dentate gyri (-).

3.4 Background for immunoprecipitation experiments

My biochemical experiments are based on IP of Ago2. Before detailing these results, it is important to summarize the results of former PhD student Balagopal Pai from the characterization and selection of Ago2 antibodies. Ago2 is part of the Argonaute (Ago) family of proteins, which bind mature miRNAs directly, and mediate miRNA-guided gene silencing. Modulation of the Ago2 protein and other components of the miRISC may be important for regulation of miRNA-mediated silencing. This form of silencing is thought to have a role in regulation of gene expression during LTP. One goal of the project was to examine regulation of Ago2, the core protein of the miRISC, after induction of LTP in the rat dentate gyrus. Ago2 antibodies from the companies Abnova, Ascenion and PTG lab were tested for detection and IP of Ago2 from total lysates of rat dentate gyrus and HEK cells overexpressing Ago2 coupled to EGFP (Figure 3.5). The antibody from Abnova was best at detecting EGFP-Ago2 and gave the greatest IP efficiency (90%) in rat dentate gyrus. The antibody from Abnova was therefore selected for further use. The EGFP-Ago2 complex expressed in HEK cells was detected at ~125 kDa in HEK cell lysate, reflecting the combined molecular mass of Ago2 (98 kDa) and EGFP (26.9 kDa).

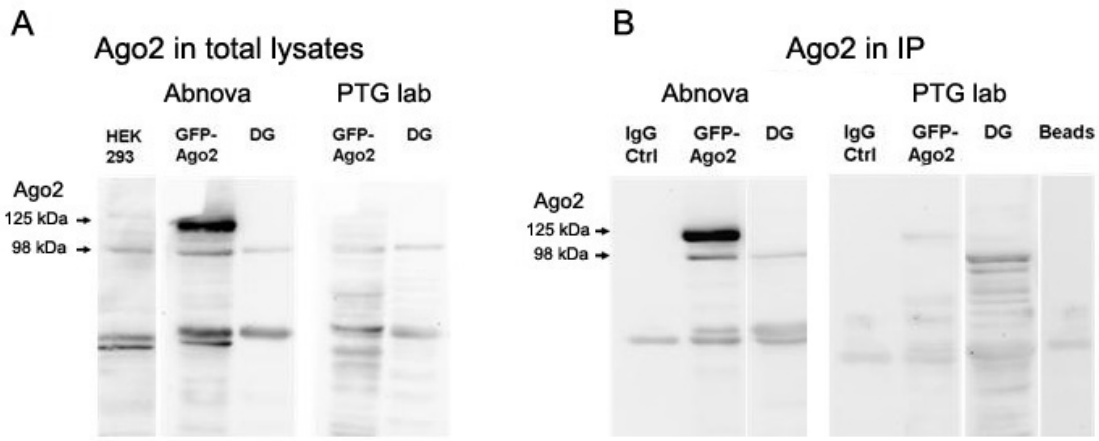

Figure 3.5 | Antibody selection for immunoprecipitation. (A) Immunoblots from total lysates probed with Ago2 antibodies from the companies Abnova and PTG lab. Ago2 was detected in naïve HEK cells, in HEK cells overexpressing EGFP-Ago2 and in dentate gyrus (DG) lysate. **(B)** Immunoblots from Ago2 IP probed with Ago2 antibodies from Abnova and PTG lab. Ago2 was detected in HEK cells overexpressing EGFP-Ago2 and in dentate gyrus lysate, but not in beads or IgG controls. Figure from Balagopal Pai.

The next step of the project was to examine proteins that interact with Ago2 in the miRISC. Co-IP of candidate RISC proteins was tested in lysates from neocortex, hippocampus proper and dentate gyrus, as well as HEK cells expressing EGFP-Ago2. The predicted proteins were the RNA helicases, DDX6 and MOV10, the RNase III enzyme, Dicer, the RNA-binding protein, FMRP, and GW182. The proteins were successfully immunoprecipitated in all lysates (Figure 3.6), although the proteins MOV10 and GW182 were inconsistently co-immunoprecipitated. There was no difference in miRISC composition between brain regions. The conditions for IP, such as protein amount, antibody concentration, incubation time and lysis buffer composition, were varied to find the optimal protocol. The retained protocol was described in the materials and methods chapter.

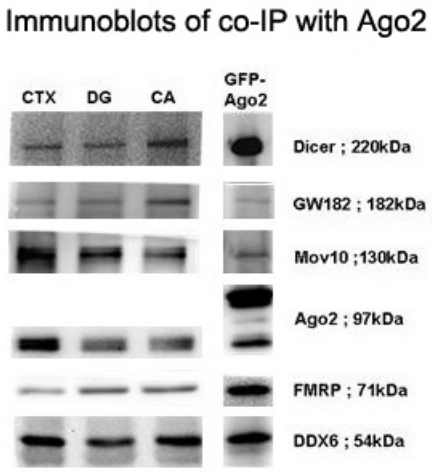

Figure 3.6 | Co-immunoprecipitation of RISC proteins with Ago2. Immunoblots showing the proteins Dicer, Gw182, MOV10, FMRP and DDX6 in Ago2 co-immunoprecipitate, in cortex, dentate gyrus, CA region and HEK cells overexpressing EGFP-Ago2. CTX, cortex; DG, dentate gyrus; CA, cornu ammonis or hippocampus proper. Figure from Balagopal Pai.

3.5 Ago2 was immunoprecipitated

Regulation of Ago2 after HFS-treatment of the dentate gyrus was examined. In the total lysates, there was a non-significant tendency for increased protein quantity of Ago2 in HFS-treated dentate gyrus, with a fold change of ~1.1 for the 30 min time point and ~1.2 for the 2 hrs times point (Figure 3.7 A, B). IP of Ago2 was performed from total lysates, and the Ago2 protein was detected by Western blotting (Figure 3.7 C, D). No change in protein expression was detected in immunoprecipitated samples. There was no significant difference between the amounts of Ago2 in the lysates and in the IP. EGFP-Ago2 expressed in HEK cells was used as a positive control for successful Ago2 detection by immunoblotting. EGFP-Ago2 was consistently detected in immunoblots, both in total lysate and in IP. Beads coupled to Ago2 antibodies without protein lysates were included in every IP experiment, as a negative control. The negative control ensured that the different antibodies used for immunoblotting did not detect the G-sepharose beads used for IP.

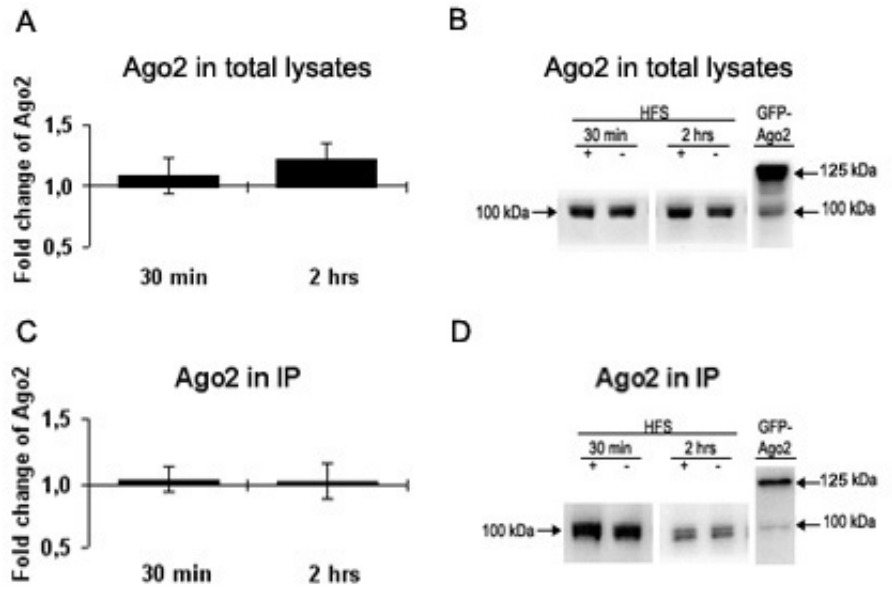

Figure 3.7 | Ago2 in total lysates and IP. (A) Column chart representing fold change (± SEM) of Ago2 content in total lysate of HFS-treated dentate gyri (+), compared to the unstimulated dentate gyri (-). Average densitometric values from immunoblots were used to create the chart. Fold change for the 30 min time point: 1.09 ± 0.15, n = 8, p = 0.82. Fold change for the 2 hrs time point: 1.23 ± 0.13, n = 5, p = 0.93. **(B)** Representative immunoblots showing Ago2 in total lysate. **(C)** Column chart representing fold change (± SEM) of Ago2 in Ago2 IP from HFS-treated dentate gyri (+), compared to the unstimulated dentate gyri (-). Fold change for the 30 min time point: 1.03 ± 0.10, n = 8, p = 0.59. Fold change for the 2 hrs time point: 1.02 ± 0.14, n = 5, p = 0.81. **(D)** Representative immunoblots showing Ago2 in IP. SEM, standard error of the mean.

3.6 Co-immunoprecipitation of Ago2-interacting proteins

Proteins predicted to interact with Ago2 were examined by co-IP. The results of these experiments are reported in this section.

3.6.1 DDX6 was associated with Ago2

DEAD box polypeptide 6 (DDX6) is an RNA helicase localized to P-bodies and stress granules. DDX6 interacts with Ago2, and is required for miRNA-induced gene silencing. DDX6 association with Ago2 after LTP induction was investigated. DDX6 was indeed co-immunoprecipitated with Ago2, both in HFS-treated dentate gyri and in the unstimulated dentate gyri. For both time points, the amount of DDX6 protein in total lysate did not change (Figure 3.8 A, B), whereas the amount of DDX6 in co-IP decreased non-significantly, with a fold change of ~0.8 for both time points (Figure 3.8 C, D). HEK cells transfected with EGFP-Ago2 were used as a positive control for successful detection of DDX6 in total lysate and as a control for successful IP.

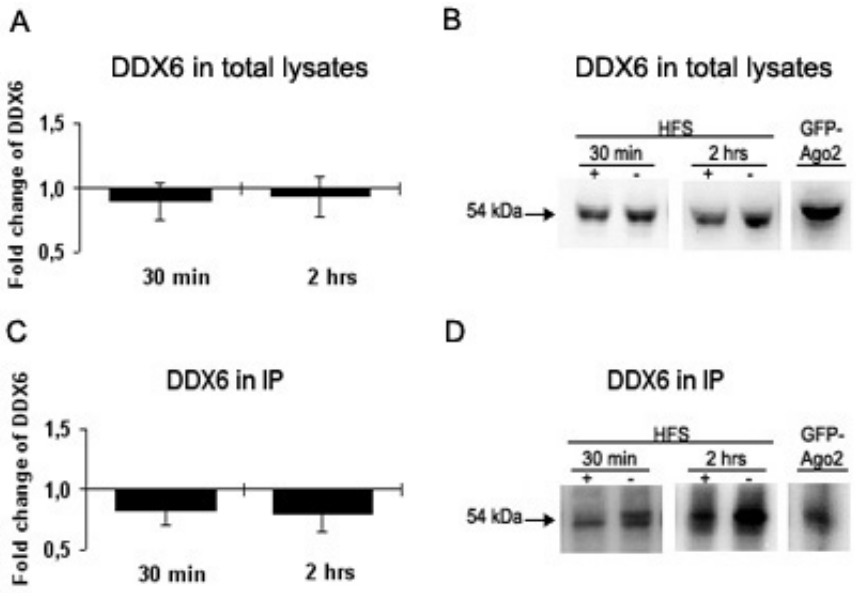

Figure 3.8 | DDX6 in total lysates and IP. (A) Fold change (± SEM) of DDX6 in total lysate of HFS-treated dentate gyri (+), compared to the unstimulated dentate gyri (-). Fold change for the 30 min time point: 0.89 ± 0.14, n = 6, p = 0.44. Fold change for the 2 hrs time point: 0.93 ± 0.16, n = 6, p = 0.88. **(B)** Representative immunoblots showing DDX6 in total lysate. **(C)** Fold change (± SEM) of DDX6 in Ago2 IP from HFS-treated dentate gyri (+), compared to the unstimulated dentate gyri (-). Representative immunoblots showing DDX6 in IP. Fold change for the 30 min time point: 0.82 ± 0.12, n = 9, p = 0.19. **(D)** Fold change for the 2 hrs time point: 0.80 ± 0.15, n = 5, p = 0.51.

3.6.2 MOV10 was detected in total lysates but not in Ago2 IP

Moloney leukemia virus 10 protein (MOV10) is an RNA helicase that binds to Ago2. MOV10 is implicated in miRNA-mediated translational repression. MOV10 may dissociate from the miRISC after synaptic activity, relieving miRISC-mediated translational repression. MOV10 was detected in total lysate, and there was a non-significant tendency for decrease in MOV10 protein quantity in HFS-treated dentate gyri, with a fold change of ~0.85 for both time points, indicating a possible degradation of MOV10 (Figure 3.9 A). MOV10 was not detected in co-IP with Ago2, but was detected in HEK cells expressing EGFP-Ago2 (positive control). Immunoblots of total lysates probed for MOV10 protein gave two bands: an invariable band at 150 kDa and a variable lower band at 130 kDa used for quantification. The lower band was chosen because several studies have detected MOV10 at 130 kDa instead of its actual molecular mass of 114 kDa, perhaps because of post-translational modifications (Banerjee et al., 2009; Meister et al., 2005). In the positive control, MOV10 was detected at 114 kDa (Figure 3.9 B).

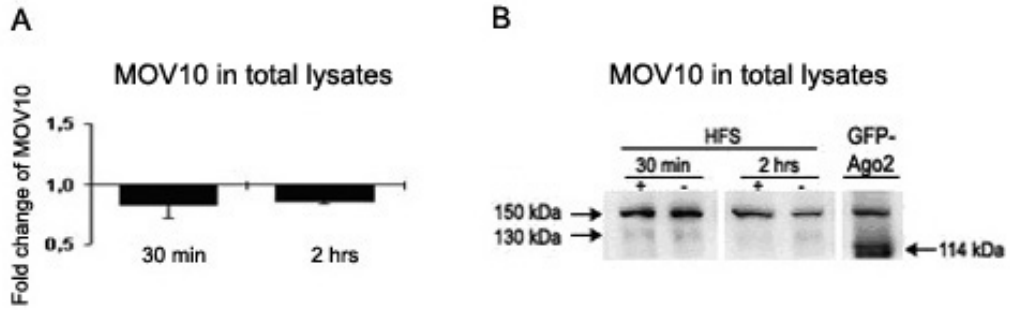

Figure 3.9 | MOV10 in total lysates. (A) Fold change of MOV10 quantity in total lysate of HFS-treated dentate gyri. Fold change for the 30 min time point: 0.83 ± 0.11, n = 6, p = 0.67. Fold change for the 2 hrs time point: 0.86 ± 0.02, n = 6, p = 0.30. **(B)** Representative immunoblots showing MOV10 in total lysate. The band used for quantification was the lower band at 130 kDa.

3.6.3 Dicer was detected in total lysates

Dicer is an RNase III enzyme involved in the cleavage of pre-miRNA in the canonical miRNA biogenesis pathway. Dicer was successfully detected in total lysates, but did not show any significant change in expression during LTP, neither at 30 min nor 2 hrs post-HFS (Figure 3.10). Dicer was not consistently detected in the co-IP with Ago2, but was always detected in HEK cells expressing EGFP-Ago2 (positive control).

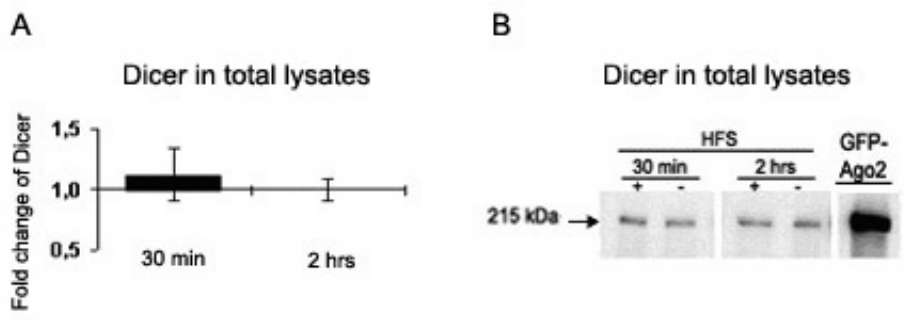

Figure 3.10 | Dicer in total lysates. (A) Fold change of Dicer in total lysate of HFS-treated dentate gyri. Fold change for the 30 min time point: 1.12 ± 0.22, n = 7, p = 0.90. Fold change for the 2 hrs time point: 1.0 ± 0.1, n = 3, p = 0.89. **(B)** Representative immunoblots showing Dicer in total lysate.

3.6.4 FMRP was difficult to detect in total lysates

Fragile-X mental retardation protein (FMRP) is an RNA-binding protein, whose absence causes fragile-X syndrome. FMRP is localized to dendrites and synapses and is thought to function as a translational repressor of specific mRNAs, including several mRNAs involved in synaptic plasticity. FMRP interacts with RISC proteins such as Ago2 and Dicer, and associates with miRNAs, but may not be essential for RNAi-mediated mRNA degradation. FMRP was difficult to detect in total lysate, showing only weak bands, even when large amounts of total protein were used (1 mg). There was no change of FMRP expression in the total lysate (Figure 3.11). In the immunoblot for co-IP, a weak band of 70-80 kDa, corresponding to the molecular mass of FMRP, was inconsistently detected. FMRP was readily detectable in HEK cells overexpressing Ago2-GFP, both for total lysate and co-IP.

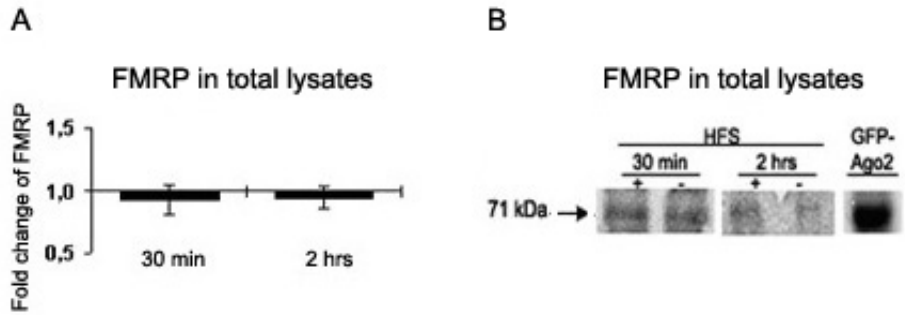

Figure 3.11 | FMRP in total lysates. (A) Fold change of FMRP in total lysate of HFS-treated dentate. Fold change for the 30 min time point: 0.92 ± 0.12, n = 8, p = 0.28. Fold change for the 2 hrs time point: 0.94 ± 0.09, n = 7, p = 0.61. **(B)** Representative immunoblots showing FMRP in total lysate.

3.6.5 GW182 in total lysates was not significantly modulated during LTP

Glycine-tryptophan proteins of 182 kDa (GW182) are required for miRNA-mediated silencing. GW182 proteins are known to interact with Ago2 and to inhibit translation, for example by interfering with the function of poly(A)-binding protein (PABP) and by interacting with deadenylase complexes. In total lysate, there was a non-significant trend for increase in GW182 protein quantity 2 hrs after the induction of LTP, with a fold change of 1.15 (Figure 3.12). GW182 was not reliably detected in co-IP with Ago2. Antibodies from two companies were tested for detection of GW182 on immunoblots. The antibody from Santa Cruz Biotechnology gave very weak bands, whereas the antibody from Bethyl laboratories gave many unspecific bands. The antibody from Bethyl laboratories was chosen because it gave the strongest band at 182 kDa, the molecular mass of GW182.

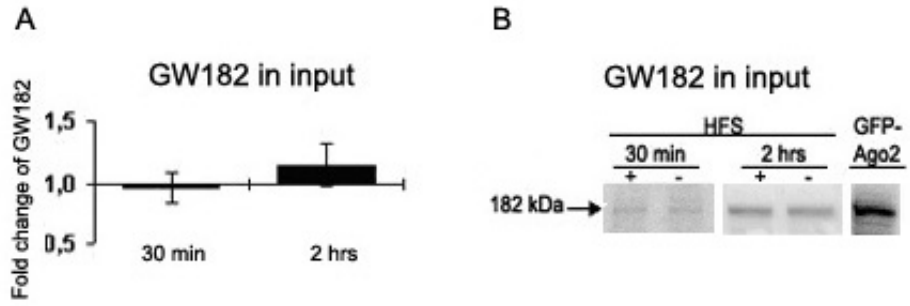

Figure 3.12 | GW182 in total lysates. (A) Fold change of GW182 quantity in total lysate of HFS-treated dentate gyri. Fold change for the 30 min time point: 0.96 ± 0.13, n = 8, p = 0.98. Fold change for the 2 hrs time point: 1.15 ± 0.17, n = 7, p = 0.80. **(B)** Representative immunoblots showing GW182 in total lysate.

3.7 Ago2 binding partners were detected by mass spectrometry

Proteins bound to Ago2 in Ago2 IP were separated by SDS-PAGE for 15 min, and the protein-containing portion of the gel was excised and cut into pieces. The proteins in the gel were reduced, alkylated and trypsinated. The resulting peptides were extracted from the gel, and were analyzed by an Orbitrap mass spectrometer. The obtained peptides were matched against the Swissprot protein database using the mascot search engine, to uncover which proteins were present in the samples. Five pairs of samples were analyzed: five HFS-treated dentate gyri, and the corresponding five untreated contralateral dentate gyri. All the samples were from experiments recorded for 30 min post-HFS. Up- or downregulated proteins in HFS-treated dentate gyri could be identified by mass spectrometry analysis.

The immunoprecipitated protein Ago2 was found in the IP samples, confirming successful IP. In two of the samples, Ago2 was neither up- nor downregulated (Figure 3.13). In sample number 2, there was a 0.17 fold change of Ago2 content in HFS-treated dentate gyri compared to the untreated dentate gyri. In sample number 4, there was a 0.76 fold change, and in sample number 5, there was a 1.60 fold change. The average fold change for all samples was 0.90 ± 0.23.

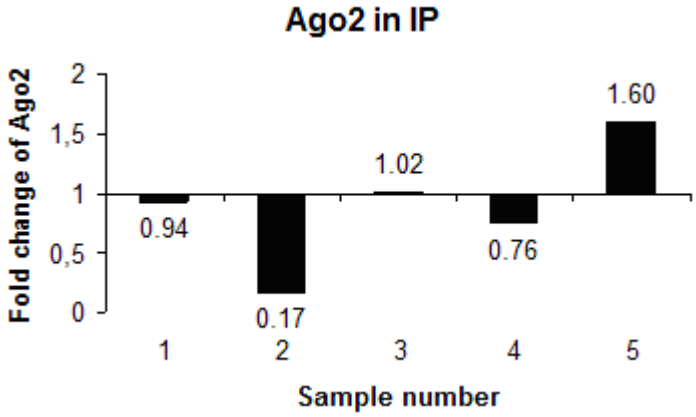

Figure 3.13 | Ago2 in IP, detected by mass spectrometry. Column chart representing fold change of Ago2 quantity in Ago2 IP from HFS-treated dentate gyri (30 min time point), compared to the unstimulated contralateral side. Average fold change for all samples: 0.90 ± 0.23.

None of the candidate binding partners of Ago2 that this thesis focuses on were detected by mass spectrometry, but the proteins DEAD box polypeptide 1 (DDX1) and fragile-X mental retardation syndrome-related protein 1 (FXR1) were detected. DDX1 belongs to the same family of DEAD (Asp-Glu-Ala-Asp) box ATP-dependent RNA helicases as DDX6. FXR1 is an RNA binding protein that interacts with the structurally and functionally similar protein FMRP (Zhang et al., 1995). Interestingly, PABP1 was found in the samples. PABP1 interacts with eIF4F and the poly(A) tail of mRNAs to protect them from silencing and degradation. Other proteins of interest were detected, such as several heterogeneous nuclear ribonucleoproteins (HNRPs), the α- and β-subunits of CaMKII, several types of PKC, and MAPK 3. None of the more than one thousand detected proteins were consistently up- or downregulated in the HFS-treated dentate gyri, compared to the unstimulated contralateral sides.

4 Discussion

LTP requires both *de novo* protein synthesis and protein degradation. Major regulators of translation are miRNAs, which act through the miRISC. This project assesses the poorly known RISC protein composition and its regulation. Findings and implications, as well as methodological considerations and future perspectives, are discussed in this chapter.

4.1 Detection of predicted Ago2 binding partners by IP

4.1.1 Ago2 may not be up- or downregulated during LTP

The protein Ago2 is the core component of miRISC. Ago2 binds miRNAs and recruits proteins that mediate gene silencing. One means by which miRNA activity could be modulated during LTP is through changes in the Ago2 association with miRNAs or with the effector RISC. miRNAs are regulated by mGluR and NMDAR signaling during LTP in rat dentate gyrus *in vivo,* at 2 hrs post-HFS (Wibrand et al., 2010). Induction of LTP in the rat dentate gyrus triggers rapid changes in Ago2-associated miRNA (Pai et al., 2012). Ago2 may be post-transcriptionally modified, altering its function. Hydroxylation and Ser387 phosphorylation stabilize Ago2 and increase Ago2 localization to P-bodies *in vitro* (Qi et al., 2008; Zeng et al., 2008). Ubiquitylation and subsequent proteasomal degradation of Ago2 lead to impaired miRNA-mediated silencing (Rybak et al., 2009). Tyr529 phosphorylation of Ago2 reduces its binding to miRNAs (Rudel et al., 2011). A study in HEK293 cells shows a small increase in mRNA levels after Ago2 knockdown. The authors found no evidence for activation of silenced genes at the mRNA level, suggesting that miRNAs have a tuning role in regulation of gene expression (Schmitter et al., 2006).

The protein composition of the RISC may be different at various stages of LTP. The critical time period for protein synthesis lasts less than one hour in most synapses. Therefore, the expression of Ago2 in the present study was investigated at two time points, namely 30 min and 2 hrs post-HFS. At 2 hrs post-HFS, it was found that Ago2 was non-significantly upregulated by ~20% in total lysates of HFS-treated dentate gyri, compared to the untreated contralateral dentate gyri. When Ago2 was immunoprecipitated from the total lysate, this tendency for Ago2 upregulation during LTP was not found. This finding could mean that protein synthesis during LTP is not controlled by differential expression of Ago2, but rather by regulation of other RISC proteins or by regulation of miRNA biogenesis. HFS-LTP is

NMDAR-dependent; it is therefore possible that NMDAR signaling during LTP regulates the pool of miRNAs available for Ago2 binding, and thus regulates which pool of mRNAs are translated or repressed. Another major mechanism of regulation not directly examined here is post-transcriptional modification of Ago and other RISC proteins. There was no significant difference between Ago2 expression in total lysates and Ago2 expression in IPs. Minor differences could perhaps be explained by modifications of Ago2, such as phosphorylation or ubiquitylation, masking the epitope. A monoclonal antibody was used for IP and immunoblotting, minimizing unspecific binding. The expression of Ago2 could be different at a later time point than 2 hrs; although a recent study in our lab shows no change in Ago2 expression 4 hrs post-HFS (Pai et al., 2012). The expression of Ago2 could be altered at an earlier time point of critical protein synthesis than 30 min, which remains to be investigated.

4.1.2 DDX6 is associated with Ago2

The RNA helicase DDX6 is a component of the RISC known to interact with Ago2. DDX6 is required for miRNA-induced translational repression (Chu and Rana, 2006). RNA helicases catalyze unwinding or remodeling of RNAs. Helicase activity may be important for assembly of the RISC and for binding or dissociation of mRNA targets (Robb and Rana, 2007; Tomari et al., 2004). DDX6 has been implicated both in increased and decreased mRNA translation, suggesting that DDX6 has a role in balancing activation and repression of translation, as proposed by Minshall et al. (2009). DDX6 proteins are localized to P-bodies and stress granules, sites of miRNA-mediated mRNA silencing. DDX6 could be the effector molecule that shuttles miRISC target mRNAs toward P-bodies, for storage or processing. Location of the miRISC to P-bodies may be the consequence rather than the cause of translation repression (Chu and Rana, 2006). The P-body marker DDX6 and the transport ribonucleoprotein (RNP) marker zipcode-binding protein 1 (ZBP1) do not colocalize in cultured hippocampal neurons, but interact in a dynamic manner via docking. Chemical stimulation of the neurons with BDNF or NMDA leads to a considerable decrease in P-bodies, suggesting that P-bodies disassemble after synaptic stimulation. Synaptic activity may lead to release of dendritically localized mRNAs from P-bodies, and possibly translation of those mRNAs (Zeitelhofer et al., 2008).

In total lysates, DDX6 expression was not altered during LTP, neither at 30 min nor 2 hrs post-HFS. DDX6 association with Ago2 was confirmed by co-IP, as found in previous studies. DDX6 was non-significantly dissociated from Ago2 during LTP, at both time points. The results from co-IP indicate that ~20% of Ago2-bound DDX6 was dissociated from Ago2

during LTP, but the results from total lysates suggest that DDX6 was not degraded. Perhaps a specific set of mRNAs, recognized by the miRISC, is relieved from repression and P-body localization in a reversible manner during LTP. The derepressed mRNAs could code for proteins specifically expressed during LTP. It is possible that DDX6 dissociation from Ago2 leads to derepression, for instance by hindering mRNA localization to P-bodies. DDX6 association with Ago2 was the same at 30 min and 2 hrs post-HFS, perhaps indicating that depression is maintained during the critical period of LTP consolidation. An example of a protein derepressed during the critical period of LTP consolidation is Arc. Arc is a protein known to be required for stable LTP expression 2 hrs after LTP induction, but is no longer required 4 hrs after LTP induction (Messaoudi et al., 2007).

4.1.3 MOV10 may be degraded during LTP

Like DDX6, MOV10 is an RNA helicase associated with P-bodies, and is involved in translational control. MOV10 is known to interact with Ago2 to mediate miRNA-induced translational repression in human cells (Meister et al., 2005). NMDAR-mediated synaptic activity promotes MOV10 ubiquitylation and subsequent degradation by the proteasome. MOV10 dissociation from the RISC may relieve miRISC-mediated translational repression (Banerjee et al., 2009). Protein degradation through the ubiquitin-proteasome system may be essential for long-term fear memory in the rat amygdala, and may be involved in several aspects of learning-induced synaptic plasticity. Fear conditioning induces NDMAR-dependent polyubiquitylation and degradation of MOV10 and other proteins involved in translational control (Jarome et al., 2011).

MOV10 was detected in total lysate, but was not found to interact with Ago2 in the rat dentate gyrus in co-IP experiments. There was a non-significant tendency for downregulation of ~15% of MOV10 proteins in the total lysate of LTP-induced dentate gyri, both 30 min and 2 hrs post-HFS. The observed downregulation of MOV10 in total lysates may be caused by MOV10 degradation as a result of NMDAR signaling during LTP, in agreement with the studies by Banerjee et al. (2009) and Jarome et al. (2011). MOV10 could be degraded through the ubiquitin-proteasome system. Perhaps MOV10 was not found in co-IP with Ago2 because MOV10 is not or weakly associated with Ago2 in the rat dentate gyrus. Alternatively, MOV10 could dissociate from Ago2 at an earlier time point than 30 min post-HFS, and not reassociate, or reassociate at a later time point than 2 hrs post-HFS. MOV10 degradation or dissociation from Ago2 may lead to derepression of translation of certain mRNAs involved in synaptic plasticity. The expression of MOV10 during LTP was similar at 30 min and 2 hrs

post-HFS, again indicating that silencing of some mRNAs may be relieved up to 2 hrs after LTP induction.

4.1.4 Dicer does not reliably co-immunoprecipitate with Ago2

The RNase III enzyme Dicer is involved in the cleavage of pre-miRNA in the canonical miRNA biogenesis pathway. Dicer interacts with Ago2, Hsp90 and TRBP, forming the miRISC loading complex (miRLC) (Liu et al., 2012). Ago2 bound to mature miRNA constitutes the minimal RISC and may subsequently dissociate from Dicer and TRBP. The protein Lin-28 regulates Dicer-mediated processing through a conserved mechanism. Lin-28 binds to let-7 pre-miRNAs and recruits an uridyl transferase (TUTase), which polyuridylates let-7 pre-miRNAs. Dicer binds to polyuridylated let-7 pre-miRNAs, and is repressed (Treiber et al., 2012). Pre-miRNAs and Dicer mRNA compete for nuclear export through Exportin 5, and Dicer is downregulated by excessive pre-miRNAs expression (Bennasser et al., 2011). An miRNA precursor deposit complex (miPDC) may serve as a temporary storage site for pre-miRNAs in the cytosol during variations in Dicer availability (Liu et al., 2012).

Dicer was detected in total lysate, but Dicer expression did not change at 30 min or 2 hrs after LTP induction. Co-IP experiments demonstrated that Dicer did not interact with Ago2 in the rat dentate gyrus. It is possible that NMDAR-dependent or -independent regulatory steps at the level of miRNA processing regulate the pool of miRNAs available for miRISC assembly during LTP. The expression of Dicer was not altered after the induction of LTP, suggesting that cleavage of pre-miRNAs by Dicer may not be the critical regulatory step of miRNA processing. Perhaps miRNA processing, miRNA loading onto the RISC, and miRISC function are controlled by other mechanisms than regulation of Dicer expression. The competition of Dicer and pre-miRNAs for export through Exportin 5 may regulate pre-miRNA availability in the cytosol. If regulation of miRNA processing is important for LTP, the regulation may focus on the selection of miRNAs necessary for LTP, and not on the expression of processing enzymes themselves. Dicer expression during LTP was the same 30 min and 2 hrs post-HFS, indicating that processing of miRNAs is perhaps not regulated by a change in Dicer availability. Indeed, pre-miRNAs could be stored in miPDCs in the cytosol, as suggested by Liu et al. (2012). An explanation for not detecting Dicer in co-IP with Ago2 might be that Dicer only briefly associates with Ago2 during the loading step of miRISC formation, and then quickly dissociates.

4.1.5 FMRP does not reliably co-immunoprecipitate with Ago2

The RNA-binding protein FMRP is localized to dendrites and synapses and is thought to function as a translational repressor of specific mRNAs, including several mRNAs involved in synaptic plasticity. FMRP may also function in mRNA stability and transport. mGluR activation is thought to regulate FMRP phosphorylation, which in turn regulates translation of different mRNAs. FMRP-dependent changes in spine morphology and AMPAR internalization can lead to mGluR-LTD. FMRP probably has multiple roles in translation. FMRP is associated with cytoplasmic fragile-X mental retardation interacting protein 1 (CYFIP1), which interacts with eIF4E and PABP in the brain. A study in the mouse brain shows that the CYFIP-FMRP complex dissociates from eIF4E, thus allowing translation in response to stimulation with BDNF or the group I mGluR agonist (S)-3,5-dihydroxy-phenylglycine (DHPG). The authors propose that CYFIP1 mediates FMRP function (Napoli et al., 2008). It is unclear whether FMRP phosphorylation regulates this mechanism. Although FMRP associates with miRNA and RISC proteins such as Ago2 and Dicer, it may not influence RISC function, but rather control the fate of translationally repressed mRNAs. FMRP and the RISC associate to distinct pools of mRNAs and the mRNAs associated with FMRP are destined to stress granules (Didiot et al., 2009). A study showed that mGluR-dependent LTD was enhanced in *fmr1* knockout mice, whereas NMDAR-dependent LTD and LTP were not affected by FMRP deficiency (Bear et al., 2004). Conversely, two more recent studies showed that NMDAR-dependent LTP in the dentate gyrus was diminished in *fmr1* knock-out mice (Eadie et al., 2012; Yun and Trommer, 2011).

FMRP was difficult to detect in total dentate gyrus lysates. FMRP is known to be found in the brain, so perhaps post-translational modifications or binding partners masked the epitope for antibody recognition. LTP induction did not affect FMRP expression in the dentate gyrus compared to the contralateral unstimulated dentate gyrus, neither at 30 min nor 2 hrs post-HFS. In co-IP experiments, FMRP was not associated with Ago2 at either time point. Our results indicate that FMRP expression may not be modulated by HFS. Perhaps FMRP-interacting proteins such as CYFIP are regulated rather than FMRP itself. FMRP could regulate the stability of present mRNAs without being part of the miRISC, and direct repressed mRNAs to stress granules. The lacking change of FMRP expression both 30 min and 2 hrs post-HFS support the idea that FMRP does not affect miRISC-mediated silencing. FMRP may not be associated with Ago2 in the rat dentate gyrus, or perhaps only transiently, which would explain why it was not detected in co-IP with Ago2. Previous studies suggest that FMRP has a role in LTD rather than LTP.

4.1.6 GW182 does not reliably co-immunoprecipitate with Ago2

GW182 interaction with Ago1 in the fly *Drosophila Melanogaster* is essential for miRNA-mediated translational repression (Eulalio et al., 2008). GW182 proteins promote translational repression by interfering with the function of PABP1 and by interacting with deadenylase complexes such as PAN2-PAN3 and CCR4-NOT. A study in cultured hippocampal neurons shows that BDNF-mediated protein synthesis requires the target mRNA to be repressed and in association with GW182 in P-bodies. BDNF causes GW182 to dissociate from translationally upregulated target mRNAs, and to associate with downregulated target mRNAs (Huang et al., 2012). GW182 associated with miRNAs and RISC proteins accumulate in P-bodies, perhaps as a consequence of silencing (Eulalio et al., 2009). GW182 can be post-transcriptionally modified. GW182 is phosphorylated but the role of this modification is unknown (Eystathioy et al., 2002).

GW182 was difficult to detect in total lysates. The immunoblots show a non-significant increase in GW182 expression 2 hrs after the induction of LTP. Co-IP experiments indicate that GW182 was not associated with Ago2. It is puzzling that GW182 was so difficult to detect in total dentate gyrus lysates, because GW182 is known to be found in neurons. Perhaps there was a pool of GW182 not recognized by the antibodies because of post-translational modifications or binding partners masking the epitope. Polyclonal antibodies from two companies were tested, and neither gave strong bands, supporting the idea of poor antibody binding to the epitope. The detected bands showed no significant difference in GW182 expression after LTP induction, neither 30 min nor 2 hrs post-HFS, meaning that LTP probably does not modulate the expression of GW182. It is nevertheless possible that GW182 interactions to other proteins are altered during LTP. The lacking Ago2-GW182 interaction in co-IP does not agree with several studies clearly showing GW182-Ago interaction, for example in *Drosophila Melanogaster* cells or human cells (Eulalio et al., 2008; Takimoto et al., 2009). Perhaps the GW182-Ago2 interaction is weaker in mammalian brain cells *in vivo*, than in cultured cells and other cell types. But no other tissues than brain were tested in this thesis, so these assertions are only speculations.

4.2 Detection of Ago2 binding partners by mass spectrometry

Proteins bound to Ago2 in Ago2 IP were detected by mass spectrometry. Proteins of interest were DDX1 and FXR1, which are homologs of respectively DDX6 and FMRP. In addition, PABP and hnRNP K were detected.

4.2.1 Ago2

Immunoprecipitated Ago2 was analyzed by mass spectrometry to detect binding partners. Five HFS-treated dentate gyri recorded for 30 min post-HFS, and the corresponding untreated contralateral dentate gyri were analyzed. The Orbitrap mass analyzer was chosen because of its speed, high resolution and sensitivity. In average, Ago2 was not up- or downregulated in HFS-treated dentate gyri. Regulation of Ago2 and other proteins varied a lot from one sample to another. Often, but not always, one specific sample differed from the others. It is difficult to draw a valid conclusion about protein regulation with such great variance within five samples. Nevertheless, the finding that Ago2 expression is not regulated 30 min post-HFS matches the results from immunoblotting, suggesting that Ago2 expression is possibly not regulated by synaptic activity.

4.2.2 DDX1 and hnRNP K

DDX1 belongs to the same family of DEAD box ATP-dependent RNA helicase as DDX6. DDX1 is a homopolymeric poly(A) RNA-binding protein involved in the 3’ end processing of pre-mRNAs. DDX1 possesses RNA unwinding activity only when in complex with heterogeneous nuclear ribonucleoprotein K (hnRNP K). The DDX1-hnRNP K complex RNA unwinding activity is important in human leukemia (K562) cells. hnRNP K is a multifunctional protein involved in the regulation of transcription, translation, nuclear transport, and signal transduction. hnRNP K is a component of the heterogeneous nuclear ribonucleoprotein complexes which bind pre-mRNAs directly and facilitate mRNA biogenesis (Chen et al., 2002).

Mass spectrometry analysis revealed that the protein DDX1 and several heterogeneous nuclear ribonucleoproteins (hnRNPs) interacted with Ago2. Of specific interest was hnRNP K. As for Ago2, the mass spectrometry results for regulation of DDX1 and hnRNP K during LTP varied a lot between each sample, even when the results were normalized to Ago2. In conclusion, neither DDX1 nor hnRNP K were consistently up- or downregulated 30 min post-HFS. Therefore, regulation of DDX1 and hnRNP K expression during LTP cannot be predicted based on our current results. It is intriguing to find pre-mRNA processing

proteins such as DDX1 and hnRNP K bound to Ago2. Perhaps DDX1 and hnRNP K interact specifically with certain pre-mRNAs or mRNAs, which in turn associate with Ago2 through miRNA interactions. Co-IP of DDX6 with Ago2 clearly showed an interaction between the two proteins. It is therefore surprising that mass spectrometry did not detect DDX6 in association with Ago2. The amino acid sequence of DDX1 is ~30% identical to other DEAD box proteins, including the nine conserved DEAD box protein motifs. One of the closest relatives of DDX1 is DDX6 (Godbout et al., 2007). It is therefore possible, but not certain, that the DDX6 antibody cross-reacted with DDX1, so that DDX1 really was detected by immunoblotting instead of DDX6.

4.2.3 FXR1

The RNA binding protein FXR1 is a paralog of FMRP. Both proteins interact with Dicer and the RISC. FMRP and FXR1 interact with the miRNA pathway to play a role in eye and neural crest development in the frog *Xenopus laevi* (Gessert et al., 2010). Even though FMRP and FXR1 are similar, they have some distinct functions. FMRP has a unique neural-specific function responsible for regulating neuronal protein expression and synaptic connectivity (Coffee et al., 2010). The expression of FXR1, but not FMRP, is increased upon Dicer knockdown and the consequent reduction of miRNAs in chicken DT40 cells. This finding suggests that FXR1 is regulated by miRNAs (Cheever et al., 2010). Conversely, FXR1 also regulates miRNAs. FXR1, but not FMRP, regulates the brain-specific miRNAs miR-9 and miR-124 by forming a complex with Dicer and pre-miRNAs, resulting in elevated miR-9 and miR-124 translation (Xu et al., 2011). Ago2 is usually associated with translational repression, but surprisingly Ago2 and FXR1 bind to the AU-rich element in the 3'UTR of tumor necrosis factor α (TNFα) mRNA in HEK293 cells and human leukemia (THP-1) cells, activating TNFα translation under serum-starved conditions. An Ago2-FXR1 activation complex may exist (Vasudevan and Steitz, 2007).

FXR1 interaction with Ago2 was detected by mass spectrometry. As for Ago2, DDX1 and HNRNP K, there was high variability in FXR1 expression during LTP between each sample, indicating that FXR1 was not consistently up- or downregulated during LTP. It is possible that FXR1, but perhaps not FMRP, is associated with the Ago2 in the mammalian brain, or that FMRP is indirectly or transiently associated with Ago2. As proposed by Vasudevan and Steitz (2007), FXR1 may be part of an activation complex, in association with Ago2. The FXR1-Ago2 complex could have a role in regulation of translation in the mammalian brain. We currently do not have any evidence for regulation of FXR1 association

to Ago2 during LTP. FXR1 may form a complex with Dicer and selected pre-miRNAs, as proposed by Xu et al. (2011). This complex could regulate synaptic plasticity-specific miRNA maturation, but this remains a speculation.

4.2.4 PABP1

PABP1 is a regulator of mRNA translation and stability and is required for miRNA-mediated regulation and nonsense-mediated decay (Brook et al., 2012). PABP interacts with eIF4F, giving rise to circular mRNAs efficiently translated and protected from degradation. GW182 may hinder PABP-eIF4G interaction or reduce PABP affinity for the poly(A) tail, to interfere with PABP-dependent mRNA circularization. Thus, GW182 interferes with PABP function in mRNA stability and translation (Tritschler et al., 2010). The RNA helicase DDX3 interacts with PABP1 and eIF4E in stress granules to regulate translation in stress responses (Shih et al., 2012). PABP1 is post-translationally modified by methylation and acetylation on various sites. The PABP1 modifications may be linked to mRNP formation (Brook et al., 2012).

Mass spectrometry analysis revealed PABP1 interaction with Ago2. PABP1 is known to be involved in translation, so the finding that PABP1 is directly or indirectly associated with Ago2 suggests that it plays a role in regulation of translation in the rat dentate gyrus. As for the other proteins detected by mass spectrometry, PABP1 was not consistently up- or downregulated after LTP induction, which does not allow us to predict any changes in PABP1 association with Ago2 during LTP.

4.2.5 MOV10, Dicer, FMRP and GW182

Surprisingly, none of the candidate binding partners of Ago2 were detected my mass spectrometry. MOV10, Dicer, FMRP and GW182 were not detected by co-IP with Ago2 either, so the mass spectrometry results match the co-IPs. This finding suggests weak or no binding of the candidate proteins to Ago2, or low abundance of the candidate proteins in the rat dentate gyrus. Other parts of the brain or other organs should be tested to confirm this hypothesis. Other possible explanations are that sites of protein-protein interaction are altered by the lysis buffer during homogenization, or that epitopes are masked by interacting proteins or post-translational modifications.

4.3 Methodological considerations

4.3.1 Electrophysiology

LTP was induced in the dentate gyrus of rats by applying HFS to the medial perforant path. There are several variables to consider in electrophysiological experiments. The animals had the same living conditions and diet, and were approximately of the same age and weight. Male rats were used because the female estrus cycle affects several parameters in the hippocampus, such as increased cell proliferation and excitability (Scharfman et al., 2003; Tanapat et al., 1999). Correct dosage of urethane for anesthesia prevented death of the rat by overdosage. The placement of the electrodes is critical for stimulation and recording, and was ensured by monitoring the recorded signals. The stimulus required to obtain maximal fEPSP, and the strength of the evoked fEPSP, could vary between animals. Exclusion criteria were set to ensure minimal variability between the experiments, although individual variations cannot be completely avoided when working with live animals. Tissue damage during electrode insertion was minimized by proceeding slowly. Microdissection was performed quickly (5-6 min) on ice to avoid tissue damage due to hypoxia and nutritional deficiencies.

4.3.2 Tissue homogenization and protein determination

After microdissection, the dentate gyri were homogenized in lysis buffer. The composition of the lysis buffer used for tissue homogenization is important. A non-ionic detergent, NP-40, was used to preserve non-covalent protein-protein interactions. A protease inhibitor cocktail was added to prevent protein degradation, and an RNase inhibitor was added to protect RNase-dependent protein associations. Even if kept on ice, proteins will start degrading at room temperature. Therefore, during homogenization, the unhomogenized samples were kept in the freezer for as long as possible. Total protein concentration in lysates was determined using the BCA assay. Protein determination was performed as quickly as possible after homogenization to avoid protein degradation. Repeated freeze-thaw cycles of protein-containing samples cause damage to the proteins because of ice crystal formation. Therefore, aliquots were made if necessary, and freeze-thaw cycles were avoided. The BCA assay was chosen for protein determination because it is compatible with the detergents present in the lysis buffer. However the lysis buffer contains the reducing agent DTT. DTT reduces the Cu^{2+} ions in the working solution of the BCA assay, forming Cu^{+} ions, which give color when forming a complex with two BCA molecules. To compensate for any inaccuracies caused by DTT in the sample lysates, both samples and proteins standard should be diluted in lysis

buffer. Loading three duplicates of each standard and sample allows detection of unequal protein loading caused by for example pipetting errors.

4.3.3 Immunoprecipitation

IP was performed to isolate the core component of the RISC, Ago2. Proteins bound to Ago2 were precipitated with it, that is, *co-immunoprecipitated*. The antibody used for IP was a mouse monoclonal immunoglobulin G1 (IgG1) Ago2 antibody. Protein G sepharose beads were used because protein G has greater affinity for IgG1 mouse antibodies than protein A. The incubation time of the antigen and the antibody-bound beads varies between antigens with different binding kinetics. The optimal incubation time for my samples, giving the greatest yield of Ago2 protein detected by Western blotting, was 3 hrs. IP is a technique that enables pull-down of an entire protein complex, and not just a single protein. Protein-protein interaction can be analyzed, and the protein composition of the complex can be characterized.

4.3.4 Western blotting

Proteins were separated by SDS-PAGE in an 8% polyacrylamide gel because the molecular masses of the candidate binding partners of Ago2 were in the range of ~50-250 kDa. An 8% gel has large enough pores to separate the heaviest proteins well, while still slowing the lightest proteins down sufficiently. The SDS-PAGE was run for 2-3 hrs, until the 50 kDa proteins approached the bottom of the gel, for maximal separation of the proteins. When separating proteins by SDS-PAGE, all the samples from one set of experiments were loaded on the same gel, because densitometric values from different immunoblots may vary. Even if the fold change in LTP-induced samples compared to controls is calculated, the difference in densitometric values from blot to blot can cause small variations in the results. Equal amounts of total protein were loaded in each well, to be able to compare the amount of candidate proteins between samples. To ensure equal protein loading, the blots were probed for the housekeeping gene β-actin. Western blotting is a semi-quantitative method adequate for comparing the amount of protein between samples, but does not give an absolute value of protein quantity. A source of variation is that the bands used for densitometry were delineated manually. Large amounts of protein were used for IP, to increase the possibility to detect Ago2 binding partners. On the other hand, using too much protein for IP may conceal small differences in protein-protein interaction between the LTP-induced samples and their controls. The choice of antibodies used for Western blotting is important for an optimized detection of the proteins of interest. Monoclonal antibodies are often preferred because they

bind specifically to their antigen. A drawback is that they may bind *too* specifically, and may not recognize the epitope if the antigen has been modified, for example because of denaturation. Polyclonal antibodies are therefore useful for the detection of denatured proteins, but may give background signal. Secondary antibodies are the main cause of background signal, but thorough washing of the membranes after incubation with antibodies reduces background signal.

4.3.5 Experimental controls for immunoprecipitation

Human embryonic kidney (HEK) 293T cells expressing EGFP-Ago2 were used as a positive control for successful detection of Ago2 and Ago2-interacting proteins by immunoblotting, both for total lysates and IP samples. Thus, the Ago2-expressing HEK cells were also a positive control for successful IP. The disadvantage of this control is that both the cell type and the species are different from the samples. The miRISC composition in human embryonic kidney cells may differ from adult rat neuronal cells. The advantage is that HEK cells are easy to grow and are readily transfected.

Antibody-bound beads with no sample were used as a negative control in co-IP. This negative control ensures that the antibodies used for immunoblotting don't cross-react with the beads. The secondary antibodies used for immunoblotting are specific for both heavy and light chains of IgG. Therefore, two bands were present on the membrane, corresponding to the heavy (50 kDa) and light (25 kDa) chains of the precipitated primary antibody. The 50 kDa band could interfere with the 54 kDa protein DDX6, but the bands were well separated by SDS-PAGE, because the gels were run until the 50 kDa proteins approached the bottom of the gel.

4.3.6 Sample preparation for mass spectrometry

The immunoprecipitated samples used for mass spectrometry were digested in-gel, because the lysis buffer in the samples contained detergents. Detergents cannot be used for protein denaturation preceding in-solution digestion, because they will interfere with the MS analysis. In-gel digestion is advantageous because the electrophoresis removes low molecular mass impurities, including detergents and buffer components (Shevchenko et al., 2006). A source of error is that 15 to 50% of peptides may be lost during sample preparation for mass spectrometry, for example during destaining, by adsorption on surfaces of pipette tips and tubes, during vacuum centrifugation, during peptide extraction from the gel, and during ionization (Granvogl et al., 2007). The reduction and alkylation steps increase the

accessibility of arginine and lysine in disulfide-containing proteins. Digestion by trypsin is advantageous because it cleaves the proteins specifically at lysine and arginine residues, which have a biological distribution that gives peptides of appropriate masses for mass spectrometry analysis. The optimum pH for trypsin digestion is between 7 and 9. Ammonium bicarbonate (ABC) is therefore a suitable buffer (pH 8.1). Desalting the samples significantly improves the quality of the mass spectra because salts are a major cause of noise.

4.4 Reflection upon project goals

Goal 1: detection of predicted Ago2 binding partners by IP

The first goal was to use IP and Western blotting to investigate whether the proteins GW182, Dicer, FMRP, MOV10 and DDX6 are associated with Ago2 in the rat dentate gyrus *in vivo*, and whether these associations are modulated during LTP. All the candidate proteins were detected in total lysate, even though FMRP, GW182 and MOV10 gave weak bands on the immunoblots. Ago2 was successfully immunoprecipitated, but of all the candidate proteins known to interact with Ago2, only DDX6 was associated with it. The experiments were done many times, and a range of different conditions were tested, such as variations in the lysis buffer, in total protein amount, and incubation time at different steps. Yet, no improvement in protein detection in co-IP was achieved. Therefore, it is tempting to suggest that the interaction between Ago2 and FMRP, GW182 and MOV10 is weaker in mammalian brain cells *in vivo*, than in cultured cells. This suggestion remains a speculation, because no other tissues than brain were co-immunoprecipitated with Ago2. There was no significant modulation of DDX6 or Ago2 in co-IP during LTP, or any significant modulation of any of the candidate proteins in total lysate during LTP. Nevertheless, some tendencies for up- or downregulation were observed. These results give an indication of how the miRISC might be modulated, but a greater number of duplicates would give a more certain answer. The number of duplicates is a challenging point because the experience is expensive and time consuming. Overall, the first goal of the project was achieved, but in retrospect, we should perhaps have focused on new candidate proteins when we repeatedly couldn't detect GW182, Dicer, FMRP and MOV10 in co-IP with Ago2.

Goal 2: detection of Ago2 binding partners by mass spectrometry

The second goal was to use mass spectrometry to identify new Ago2 binding partners, and to detect changes in protein interactions during LTP. Ago2 in IP was detected by Orbitrap mass

spectrometry, confirming successful IP of Ago2. More than a thousand direct or indirect binding partners of Ago2 were detected. Of these, a few proteins important in translational silencing were found, such as PABP1, DDX1 and FXR1. No consistent changes in protein interaction with Ago2 or expression of Ago2 itself were found during LTP. The goal was achieved, but the work could be expanded. Additional replicates could give more reliable information about regulation of protein expression. Mass spectrometry could be performed for dentate gyri collected at other time points than 30 min post-HFS, to investigate whether protein regulation varies at different time points during LTP.

4.5 Conclusions and future perspectives

This study does not show any significant remodeling of the miRISC during LTP, but neither does it exclude this possibility. Remodeling of the miRISC may alter its function in translational repression, and change the expression of proteins important in synaptic plasticity. It is possible that mechanisms other than RISC remodeling, such as control of miRNA synthesis, may control changes in gene expression. Knowing the mechanisms underlying synaptic plasticity will give us a better understanding of learning and memory, and eventually, enable us to better study diseases of cognition. Many interesting questions about the miRISC in the mammalian brain are left unanswered. The full RISC protein composition is still unknown, and we have just started to investigate its modulation during LTP. Which receptors are required for RISC modulation? The cascade of events leading to changes in RISC composition is a possible field of study, and RISC localization in neurons is yet another interesting issue. Finally, the behavioral significance of RISC function needs more studying. The RISC pathway regulates synaptic protein synthesis associated with memory in *Drosophila Melanogaster* (Ashraf et al., 2006). Ago2 and the RISC may play a role in mammalian memory formation *in vivo*. In a study, small interfering RNAs (siRNAs) targeting Ago2 were injected in the dorsal hippocampus of mice. siRNA-mediated silencing of Ago2 impaired short-term memory and long-term contextual fear memory (Batassa et al., 2010). More studies are needed to investigate the possible link between RISC regulation of protein synthesis and memory formation in mammals.

Several studies could be conducted in the foreseeable future. The protein composition of the RISC during LTP could be further analyzed by mass spectrometry, at other time point than 30 min after the induction of LTP. NMDAR-dependence of RISC modulation can be tested *in vivo* by infusion of NMDAR antagonists such as AP5 or CPP into the hippocampus,

before LTP induction. The RNase dependence of protein-protein interactions can be tested by adding an RNase to the beads during IP of the miRISC. Protein interactions with Ago2 can be confirmed by immunoprecipitating candidate proteins from dentate gyrus lysate, and trying to detect Ago2 in the IP. Candidate proteins for which available antibodies are not specific enough can be expressed in mammalian cells *in vitro* and tagged with protein tags such as Flag or glutathione S-transferase (GST). The tagged proteins can be immunoprecipitated and protein-protein interactions can be analyzed by Western blotting. Other techniques for analysis of protein-protein interactions *in vitro* are fluorescence resonance energy transfer (FRET), surface plasmon resonance (SPR) and yeast-two-hybrid. Colocalization of a RISC protein to P-bodies can be analyzed by probing cells with antibodies against the protein of interest and against a marker for P-bodies, such as mRNA decapping enzyme 1A (DCD1A). Modifications of RISC proteins, such as phosphorylation or ubiquitylation, can be analyzed by Western blotting. Localization of the miRISC can be analyzed in synaptoneurosomes, which are isolated resealed pre- and postsynaptic structures. Synaptoneurosomes could be used for proteomic analysis of synaptic miRISC. Changes in miRISC protein composition could then not be attributed to proteins transported from the cell body. Sucrose gradient analysis of polysomes can reveal whether RISC proteins are present in the polysomal fraction, which would indicate a role of the miRISC in translational regulation at polysomes. miRISC function can be analyzed further by blocking the function of RISC proteins such as GW182, for example by lentiviral expression of short hairpin RNAs (shRNAs). Knockout mice of RISC proteins can be useful for behavioral studies. It would be interesting to analyze the behavioral importance of the RISC and specific RISC proteins in learning and memory.

Appendix

A User manuals

Lipofectamine™ 2000

http://tools.invitrogen.com/content/sfs/manuals/lipofectamine2000_man.pdf

Mini-PROTEAN® 3 Cell

http://www3.bio-rad.com/cmc_upload/Literature/44432/4006157B.pdf

Mini Trans-Blot® Electrophoretic Transfer Cell

http://www3.bio-rad.com/cmc_upload/Literature/13280/M1703930.pdf

Pierce® BCA Protein Assay Kit

http://www.piercenet.com/instructions/2161296.pdf

Pierce® ECL Western Blotting Substrate

http://www.piercenet.com/instructions/2161743.pdf

B Recipes

Polyacrylamide gel

	Resolving gel (8% acrylamide)	**Stacking gel (4% acrylamide)**
ddH_2O	9.5 ml	6 ml
30% Acrylamide/Bis 37.5:1	5.2 ml	1.34 ml
Tris-HCl pH 6.8	-	2.5 ml
Tris-HCl pH 8.8	5 ml	-
10% Sodium dodecyl sulfate (SDS)	160 µl	100 µl
10% Ammonium persulfate (APS)	160 µl	50 µl
TEMED	16 µl	10 µl
Total volume	~20 ml	10 ml

References

Andersen P, Morris R, Amaral D, Bliss T, O'Keefe J (2007). *The hippocampus book* New York: Oxford University Press.

Ashraf SI, McLoon AL, Sclarsic SM, Kunes S (2006). Synaptic protein synthesis associated with memory is regulated by the RISC pathway in Drosophila. *Cell* 124: 191-205

Bagni C, Greenough WT (2005). From mRNP trafficking to spine dysmorphogenesis: the roots of fragile X syndrome. *Nat Rev Neurosci* 6: 376-87

Banerjee S, Neveu P, Kosik KS (2009). A coordinated local translational control point at the synapse involving relief from silencing and MOV10 degradation. *Neuron* 64: 871-84

Bassell GJ, Warren ST (2008). Fragile X syndrome: loss of local mRNA regulation alters synaptic development and function. *Neuron* 60: 201-14

Batassa EM, Costanzi M, Saraulli D, Scardigli R, Barbato C, Cogoni C, Cestari V (2010). RISC activity in hippocampus is essential for contextual memory. *Neurosci Lett* 471: 185-8

Bear MF, Huber KM, Warren ST (2004). The mGluR theory of fragile X mental retardation. *Trends Neurosci* 27: 370-7

Bennasser Y, Chable-Bessia C, Triboulet R, Gibbings D, Gwizdek C, Dargemont C, Kremer EJ, Voinnet O, Benkirane M (2011). Competition for XPO5 binding between Dicer mRNA, pre-miRNA and viral RNA regulates human Dicer levels. *Nat Struct Mol Biol* 18: 323-7

Besse F, Ephrussi A (2008). Translational control of localized mRNAs: restricting protein synthesis in space and time. *Nat Rev Mol Cell Biol* 9: 971-80

Bliss TV, Collingridge GL (1993). A synaptic model of memory: long-term potentiation in the hippocampus. *Nature* 361: 31-9

Bliss TV, Collingridge GL, Morris RG (2003). Introduction. Long-term potentiation and structure of the issue. *Philos Trans R Soc Lond B Biol Sci* 358: 607-11

Bliss TV, Lomo T (1973). Long-lasting potentiation of synaptic transmission in the dentate area of the anaesthetized rabbit following stimulation of the perforant path. *J Physiol* 232: 331-56

Bramham CR, Alme MN, Bittins M, Kuipers SD, Nair RR, Pai B, Panja D, Schubert M, Soule J, Tiron A, Wibrand K (2010). The Arc of synaptic memory. *Exp Brain Res* 200: 125-40

Bramham CR, Messaoudi E (2005). BDNF function in adult synaptic plasticity: the synaptic consolidation hypothesis. *Prog Neurobiol* 76: 99-125

Bramham CR, Wells DG (2007). Dendritic mRNA: transport, translation and function. *Nat Rev Neurosci* 8: 776-89

Bramham CR, Worley PF, Moore MJ, Guzowski JF (2008). The immediate early gene Arc/Arg3.1: regulation, mechanisms, and function. *J Neurosci* 28: 11760-7

Brook M, McCracken L, Reddington JP, Lu ZL, Morrice NA, Gray NK (2012). The multifunctional poly(A)-binding protein (PABP) 1 is subject to extensive dynamic post-translational modification, which molecular modelling suggests plays an important role in co-ordinating its activities. *Biochem J* 441: 803-12

Broytman O, Westmark PR, Gurel Z, Malter JS (2009). Rck/p54 interacts with APP mRNA as part of a multi-protein complex and enhances APP mRNA and protein expression in neuronal cell lines. *Neurobiol Aging* 30: 1962-74

Carthew RW, Sontheimer EJ (2009). Origins and Mechanisms of miRNAs and siRNAs. *Cell* 136: 642-55

Castillo PE (2012). Presynaptic LTP and LTD of Excitatory and Inhibitory Synapses. *Cold Spring Harb Perspect Biol* 4

Cheever A, Blackwell E, Ceman S (2010). Fragile X protein family member FXR1P is regulated by microRNAs. *RNA* 16: 1530-9

Chen HC, Lin WC, Tsay YG, Lee SC, Chang CJ (2002). An RNA helicase, DDX1, interacting with poly(A) RNA and heterogeneous nuclear ribonucleoprotein K. *J Biol Chem* 277: 40403-9

Cheung TH, Cardinal RN (2005). Hippocampal lesions facilitate instrumental learning with delayed reinforcement but induce impulsive choice in rats. *BMC Neurosci* 6: 36

Chu CY, Rana TM (2006). Translation repression in human cells by microRNA-induced gene silencing requires RCK/p54. *PLoS Biol* 4: e210

Coffee RL, Jr., Tessier CR, Woodruff EA, 3rd, Broadie K (2010). Fragile X mental retardation protein has a unique, evolutionarily conserved neuronal function not shared with FXR1P or FXR2P. *Dis Model Mech* 3: 471-85

Costa FF (2010). Non-coding RNAs: Meet thy masters. *Bioessays* 32: 599-608

Didiot MC, Subramanian M, Flatter E, Mandel JL, Moine H (2009). Cells lacking the fragile X mental retardation protein (FMRP) have normal RISC activity but exhibit altered stress granule assembly. *Mol Biol Cell* 20: 428-37

Dudai Y (2004). *Memory from A to Z: keywords, concepts and beyond* pp. 198. New York: Oxford University Press.

Eadie BD, Cushman J, Kannangara TS, Fanselow MS, Christie BR (2012). NMDA receptor hypofunction in the dentate gyrus and impaired context discrimination in adult Fmr1 knockout mice. *Hippocampus* 22: 241-54

Edbauer D, Neilson JR, Foster KA, Wang CF, Seeburg DP, Batterton MN, Tada T, Dolan BM, Sharp PA, Sheng M (2010). Regulation of synaptic structure and function by FMRP-associated microRNAs miR-125b and miR-132. *Neuron* 65: 373-84

Ender C, Meister G (2010). Argonaute proteins at a glance. *J Cell Sci* 123: 1819-23

Eulalio A, Behm-Ansmant I, Izaurralde E (2007). P bodies: at the crossroads of post-transcriptional pathways. *Nat Rev Mol Cell Biol* 8: 9-22

Eulalio A, Huntzinger E, Izaurralde E (2008). GW182 interaction with Argonaute is essential for miRNA-mediated translational repression and mRNA decay. *Nat Struct Mol Biol* 15: 346-53

Eulalio A, Tritschler F, Izaurralde E (2009). The GW182 protein family in animal cells: new insights into domains required for miRNA-mediated gene silencing. *RNA* 15: 1433-42

Eystathioy T, Chan EK, Tenenbaum SA, Keene JD, Griffith K, Fritzler MJ (2002). A phosphorylated cytoplasmic autoantigen, GW182, associates with a unique population of human mRNAs within novel cytoplasmic speckles. *Mol Biol Cell* 13: 1338-51

Filipowicz W, Bhattacharyya SN, Sonenberg N (2008). Mechanisms of post-transcriptional regulation by microRNAs: are the answers in sight? *Nat Rev Genet* 9: 102-14

Fukaya T, Tomari Y (2011). PABP is not essential for microRNA-mediated translational repression and deadenylation in vitro. *EMBO J* 30: 4998-5009

Gessert S, Bugner V, Tecza A, Pinker M, Kuhl M (2010). FMR1/FXR1 and the miRNA pathway are required for eye and neural crest development. *Dev Biol* 341: 222-35

Godbout R, Li L, Liu RZ, Roy K (2007). Role of DEAD box 1 in retinoblastoma and neuroblastoma. *Future Oncol* 3: 575-87

Granvogl B, Ploscher M, Eichacker LA (2007). Sample preparation by in-gel digestion for mass spectrometry-based proteomics. *Anal Bioanal Chem* 389: 991-1002

Griffiths-Jones S (2004). The microRNA Registry. *Nucleic Acids Res* 32: D109-11

Grosshans H, Filipowicz W (2008). Molecular biology: the expanding world of small RNAs. *Nature* 451: 414-6

Grossman AW, Aldridge GM, Weiler IJ, Greenough WT (2006). Local protein synthesis and spine morphogenesis: Fragile X syndrome and beyond. *J Neurosci* 26: 7151-5

Huang YW, Ruiz CR, Eyler EC, Lin K, Meffert MK (2012). Dual regulation of miRNA biogenesis generates target specificity in neurotrophin-induced protein synthesis. *Cell* 148: 933-46

Huntzinger E, Izaurralde E (2011). Gene silencing by microRNAs: contributions of translational repression and mRNA decay. *Nat Rev Genet* 12: 99-110

Jangra RK, Yi M, Lemon SM (2010). DDX6 (Rck/p54) is required for efficient hepatitis C virus replication but not for internal ribosome entry site-directed translation. *J Virol* 84: 6810-24

Jarome TJ, Werner CT, Kwapis JL, Helmstetter FJ (2011). Activity dependent protein degradation is critical for the formation and stability of fear memory in the amygdala. *PLoS One* 6: e24349

Kawahara H, Imai T, Okano H (2012). MicroRNAs in Neural Stem Cells and Neurogenesis. *Front Neurosci* 6: 30

Krol J, Loedige I, Filipowicz W (2010). The widespread regulation of microRNA biogenesis, function and decay. *Nat Rev Genet* 11: 597-610

Kuzuoglu-Ozturk D, Huntzinger E, Schmidt S, Izaurralde E (2012). The Caenorhabditis elegans GW182 protein AIN-1 interacts with PAB-1 and subunits of the PAN2-PAN3 and CCR4-NOT deadenylase complexes. *Nucleic Acids Res*

Lee RC, Feinbaum RL, Ambros V (1993). The C. elegans heterochronic gene lin-4 encodes small RNAs with antisense complementarity to lin-14. *Cell* 75: 843-54

Li S, Lian SL, Moser JJ, Fritzler ML, Fritzler MJ, Satoh M, Chan EK (2008). Identification of GW182 and its novel isoform TNGW1 as translational repressors in Ago2-mediated silencing. *J Cell Sci* 121: 4134-44

Li Z, Rana TM (2012). Molecular Mechanisms of RNA-Triggered Gene Silencing Machineries. *Acc Chem Res*

Liu X, Jin DY, McManus MT, Mourelatos Z (2012). Precursor MicroRNA-Programmed Silencing Complex Assembly Pathways in Mammals. *Mol Cell*

Malenka RC, Bear MF (2004). LTP and LTD: an embarrassment of riches. *Neuron* 44: 5-21

Martin SJ, Grimwood PD, Morris RG (2000). Synaptic plasticity and memory: an evaluation of the hypothesis. *Annu Rev Neurosci* 23: 649-711

Medina JH, Izquierdo I (1995). Retrograde messengers, long-term potentiation and memory. *Brain Res Brain Res Rev* 21: 185-94

Meister G, Landthaler M, Peters L, Chen PY, Urlaub H, Luhrmann R, Tuschl T (2005). Identification of novel argonaute-associated proteins. *Curr Biol* 15: 2149-55

Messaoudi E, Kanhema T, Soule J, Tiron A, Dagyte G, da Silva B, Bramham CR (2007). Sustained Arc/Arg3.1 synthesis controls long-term potentiation consolidation through regulation of local actin polymerization in the dentate gyrus in vivo. *J Neurosci* 27: 10445-55

Messaoudi E, Ying SW, Kanhema T, Croll SD, Bramham CR (2002). Brain-derived neurotrophic factor triggers transcription-dependent, late phase long-term potentiation in vivo. *J Neurosci* 22: 7453-61

Minshall N, Kress M, Weil D, Standart N (2009). Role of p54 RNA helicase activity and its C-terminal domain in translational repression, P-body localization and assembly. *Mol Biol Cell* 20: 2464-72

Molnar A, Schwach F, Studholme DJ, Thuenemann EC, Baulcombe DC (2007). miRNAs control gene expression in the single-cell alga Chlamydomonas reinhardtii. *Nature* 447: 1126-9

Muddashetty RS, Nalavadi VC, Gross C, Yao X, Xing L, Laur O, Warren ST, Bassell GJ (2011). Reversible inhibition of PSD-95 mRNA translation by miR-125a, FMRP phosphorylation, and mGluR signaling. *Mol Cell* 42: 673-88

Napoli I, Mercaldo V, Boyl PP, Eleuteri B, Zalfa F, De Rubeis S, Di Marino D, Mohr E, Massimi M, Falconi M, Witke W, Costa-Mattioli M, Sonenberg N, Achsel T, Bagni C (2008). The fragile X syndrome protein represses activity-dependent translation through CYFIP1, a new 4E-BP. *Cell* 134: 1042-54

Narayanan U, Nalavadi V, Nakamoto M, Thomas G, Ceman S, Bassell GJ, Warren ST (2008). S6K1 phosphorylates and regulates fragile X mental retardation protein (FMRP) with the neuronal protein synthesis-dependent mammalian target of rapamycin (mTOR) signaling cascade. *J Biol Chem* 283: 18478-82

Neves G, Cooke SF, Bliss TV (2008). Synaptic plasticity, memory and the hippocampus: a neural network approach to causality. *Nat Rev Neurosci* 9: 65-75

Pai B, Siripornmongcolchai T, Berentsen B, Fathpour AP, Wibrand K, Bramham CR (2012). Regulation of argonaute-2-associated microRNAs during LTP in adult rat brain *in vivo*. *Manuscript*

Panja D, Dagyte G, Bidinosti M, Wibrand K, Kristiansen AM, Sonenberg N, Bramham CR (2009). Novel translational control in Arc-dependent long term potentiation consolidation in vivo. *J Biol Chem* 284: 31498-511

Peng S, Zhang Y, Zhang J, Wang H, Ren B (2011). Glutamate receptors and signal transduction in learning and memory. *Mol Biol Rep* 38: 453-60

Qi HH, Ongusaha PP, Myllyharju J, Cheng D, Pakkanen O, Shi Y, Lee SW, Peng J (2008). Prolyl 4-hydroxylation regulates Argonaute 2 stability. *Nature* 455: 421-4

Qi MY, Wang ZZ, Zhang Z, Shao Q, Zeng A, Li XQ, Li WQ, Wang C, Tian FJ, Li Q, Zou J, Qin YW, Brewer G, Huang S, Jing Q (2012). AU-rich-element-dependent translation repression requires the cooperation of tristetraprolin and RCK/P54. *Mol Cell Biol* 32: 913-28

Reinhart BJ, Slack FJ, Basson M, Pasquinelli AE, Bettinger JC, Rougvie AE, Horvitz HR, Ruvkun G (2000). The 21-nucleotide let-7 RNA regulates developmental timing in Caenorhabditis elegans. *Nature* 403: 901-6

Robb GB, Rana TM (2007). RNA helicase A interacts with RISC in human cells and functions in RISC loading. *Mol Cell* 26: 523-37

Rudel S, Wang Y, Lenobel R, Korner R, Hsiao HH, Urlaub H, Patel D, Meister G (2011). Phosphorylation of human Argonaute proteins affects small RNA binding. *Nucleic Acids Res* 39: 2330-43

Rybak A, Fuchs H, Hadian K, Smirnova L, Wulczyn EA, Michel G, Nitsch R, Krappmann D, Wulczyn FG (2009). The let-7 target gene mouse lin-41 is a stem cell specific E3 ubiquitin ligase for the miRNA pathway protein Ago2. *Nat Cell Biol* 11: 1411-20

Scharfman HE, Mercurio TC, Goodman JH, Wilson MA, MacLusky NJ (2003). Hippocampal excitability increases during the estrous cycle in the rat: a potential role for brain-derived neurotrophic factor. *J Neurosci* 23: 11641-52

Schmitter D, Filkowski J, Sewer A, Pillai RS, Oakeley EJ, Zavolan M, Svoboda P, Filipowicz W (2006). Effects of Dicer and Argonaute down-regulation on mRNA levels in human HEK293 cells. *Nucleic Acids Res* 34: 4801-15

Schratt G (2009). microRNAs at the synapse. *Nat Rev Neurosci* 10: 842-9

Shevchenko A, Tomas H, Havlis J, Olsen JV, Mann M (2006). In-gel digestion for mass spectrometric characterization of proteins and proteomes. *Nat Protoc* 1: 2856-60

Shih JW, Wang WT, Tsai TY, Kuo CY, Li HK, Wu Lee YH (2012). Critical roles of RNA helicase DDX3 and its interactions with eIF4E/PABP1 in stress granule assembly and stress response. *Biochem J* 441: 119-29

Smith PK, Krohn RI, Hermanson GT, Mallia AK, Gartner FH, Provenzano MD, Fujimoto EK, Goeke NM, Olson BJ, Klenk DC (1985). Measurement of protein using bicinchoninic acid. *Anal Biochem* 150: 76-85

Squire LR (2004). Memory systems of the brain: a brief history and current perspective. *Neurobiol Learn Mem* 82: 171-7

Steward O, Schuman EM (2001). Protein synthesis at synaptic sites on dendrites. *Annu Rev Neurosci* 24: 299-325

Steward O, Wallace CS, Lyford GL, Worley PF (1998). Synaptic activation causes the mRNA for the IEG Arc to localize selectively near activated postsynaptic sites on dendrites. *Neuron* 21: 741-51

Sutton MA, Schuman EM (2006). Dendritic protein synthesis, synaptic plasticity, and memory. *Cell* 127: 49-58

Tada T, Sheng M (2006). Molecular mechanisms of dendritic spine morphogenesis. *Curr Opin Neurobiol* 16: 95-101

Takimoto K, Wakiyama M, Yokoyama S (2009). Mammalian GW182 contains multiple Argonaute-binding sites and functions in microRNA-mediated translational repression. *RNA* 15: 1078-89

Tanaka J, Horiike Y, Matsuzaki M, Miyazaki T, Ellis-Davies GC, Kasai H (2008). Protein synthesis and neurotrophin-dependent structural plasticity of single dendritic spines. *Science* 319: 1683-7

Tanapat P, Hastings NB, Reeves AJ, Gould E (1999). Estrogen stimulates a transient increase in the number of new neurons in the dentate gyrus of the adult female rat. *J Neurosci* 19: 5792-801

Tomari Y, Du T, Haley B, Schwarz DS, Bennett R, Cook HA, Koppetsch BS, Theurkauf WE, Zamore PD (2004). RISC assembly defects in the Drosophila RNAi mutant armitage. *Cell* 116: 831-41

Treiber T, Treiber N, Meister G (2012). Regulation of microRNA biogenesis and function. *Thromb Haemost* 107

Tritschler F, Huntzinger E, Izaurralde E (2010). Role of GW182 proteins and PABPC1 in the miRNA pathway: a sense of deja vu. *Nat Rev Mol Cell Biol* 11: 379-84

Vasudevan S, Steitz JA (2007). AU-rich-element-mediated upregulation of translation by FXR1 and Argonaute 2. *Cell* 128: 1105-18

Wang X, Han Y, Dang Y, Fu W, Zhou T, Ptak RG, Zheng YH (2010). Moloney leukemia virus 10 (MOV10) protein inhibits retrovirus replication. *J Biol Chem* 285: 14346-55

Wang Y, Juranek S, Li H, Sheng G, Tuschl T, Patel DJ (2008). Structure of an argonaute silencing complex with a seed-containing guide DNA and target RNA duplex. *Nature* 456: 921-6

Wibrand K, Panja D, Tiron A, Ofte ML, Skaftnesmo KO, Lee CS, Pena JT, Tuschl T, Bramham CR (2010). Differential regulation of mature and precursor microRNA expression by NMDA and metabotropic glutamate receptor activation during LTP in the adult dentate gyrus in vivo. *Eur J Neurosci* 31: 636-45

Xu XL, Zong R, Li Z, Biswas MH, Fang Z, Nelson DL, Gao FB (2011). FXR1P but not FMRP regulates the levels of mammalian brain-specific microRNA-9 and microRNA-124. *J Neurosci* 31: 13705-9

Yun SH, Trommer BL (2011). Fragile X mice: reduced long-term potentiation and N-Methyl-D-Aspartate receptor-mediated neurotransmission in dentate gyrus. *J Neurosci Res* 89: 176-82

Zalfa F, Giorgi M, Primerano B, Moro A, Di Penta A, Reis S, Oostra B, Bagni C (2003). The fragile X syndrome protein FMRP associates with BC1 RNA and regulates the translation of specific mRNAs at synapses. *Cell* 112: 317-27

Zeitelhofer M, Karra D, Macchi P, Tolino M, Thomas S, Schwarz M, Kiebler M, Dahm R (2008). Dynamic interaction between P-bodies and transport ribonucleoprotein particles in dendrites of mature hippocampal neurons. *J Neurosci* 28: 7555-62

Zeng Y, Sankala H, Zhang X, Graves PR (2008). Phosphorylation of Argonaute 2 at serine-387 facilitates its localization to processing bodies. *Biochem J* 413: 429-36

Zhang Y, O'Connor JP, Siomi MC, Srinivasan S, Dutra A, Nussbaum RL, Dreyfuss G (1995). The fragile X mental retardation syndrome protein interacts with novel homologs FXR1 and FXR2. *EMBO J* 14: 5358-66